A Resource Assessment of Copper and Nickel Sulfides within the Mountain View Area of the Stillwater Complex, Montana

U.S. GEOLOGICAL SURVEY BULLETIN 1674–B

Chapter B

A Resource Assessment of Copper and Nickel Sulfides within the Mountain View Area of the Stillwater Complex, Montana

By E. D. ATTANASI and W. J. BAWIEC

U.S. GEOLOGICAL SURVEY BULLETIN 1674

CONTRIBUTIONS ON ORE DEPOSITS IN THE EARLY MAGMATIC ENVIRONMENT

DEPARTMENT OF THE INTERIOR
DONALD PAUL HODEL, Secretary

U.S. GEOLOGICAL SURVEY
Dallas L. Peck, Director

UNITED STATES GOVERNMENT PRINTING OFFICE: 1987

For sale by the Books and Open-File Reports Section, U.S. Geological Survey, Federal Center, Box 25425, Denver, CO 80225

Library of Congress Cataloging in Publication Data

Attanasi, E. D.
A resource assessment of copper and nickel sulfides within the Mountain View area of the Stillwater Complex, Montana.
(Contributions on ore deposits in the early magmatic environment ; B) (Geological Survey bulletin ; 1674–B)
Bibliography: p.
Supt. of Docs. no.: I 19.3:1674–B
1. Copper sulphide—Montana. 2. Nickel sulphide. I. Bawiec, W. J. II. Title. III. Series. IV. Series: U.S. Geological Survey bulletin ; 1674–B.
QE75.B9 no. 1674–B 557.3 s 86–600027
[QE390.2.C6] [553.4'3'09786] Rev.

The use of trade names in this publication is for identification only and does not constitute endorsement by the U.S. Geological Survey.

CONTENTS

FIGURES

TABLES

A Resource Assessment of Copper and Nickel Sulfides within the Mountain View Area of the Stillwater Complex, Montana

By E. D. Attanasi *and* W. J. Bawiec

Abstract

Drill-hole data within the Mountain View area of the Stillwater Complex are used to identify specific lithologies and locations that could contain commercial-grade copper and nickel ore. In addition to outcrops containing sulfide mineralization, the Mountain View area has been penetrated by over 110 drill holes whose associated cores have been recovered and analyzed for concentrations of copper and nickel.

The area southwest of the Verdigris fault in the Mountain View area was intensively studied and found to be composed of conterminous fault-bounded blocks. Concentration statistics for copper and nickel based on drill-hole data were computed for 100-foot horizontal intervals within individual stratigraphic units for the entire area. The resulting grade estimates were lower than those for currently operating underground copper and nickel mines.

Data on both copper and nickel concentrations were analyzed by individual fault-bounded blocks and examined in 25-foot intervals both above the base of the Basal series and below the Basal series into the metasedimentary rocks. Copper and nickel grades tend to decline as distance both above and below this stratigraphic contact increases. The location of potentially commercial-grade ore was demonstrated.

Only two fault-bounded blocks contained enough data for estimating grade-tonnage (in situ tonnage) relationships. The fault block immediately west of the Verdigris fault contains 17.1 to 22.3 million short tons of ore having an average grade of 0.5 percent combined copper and nickel. In the other fault-bounded block studied, which is located farther west, estimated tonnage is 2.4 to 5.3 million short tons of ore, also having an average grade of 0.5 percent combined copper and nickel. These estimates are of in situ material and do not allow for losses in mining and metallurgical recovery.

The tonnage estimates are based on relatively sparse data and should be regarded as uncertain. In order to reduce this uncertainty, additional sampling and verification of estimates are needed. If the additional tonnage of other fault-bounded blocks is required for a minimum commercial size operation, then future drilling should be focused on establishing the continuity of mineralization within the lithologic units lying directly above and below the contact between the Basal series and metasedimentary rocks in these other blocks.

INTRODUCTION

Drill-hole data containing copper and nickel concentrations in the Mountain View area of the Stillwater Complex, Montana, are examined in order to identify specific lithologies and areas that could contain copper and nickel ore. The term "ore" as used in this study refers to copper- and nickel-enriched rocks and is not restricted to rocks that can currently be mined at a profit. According to current geologic interpretation, copper and nickel sulfides are concentrated within the lowermost igneous units of the Stillwater Complex (Page, 1979) and are also frequently associated with sills and dikes intruding the adjacent metasedimentary rocks (Zientek, 1983). As shown in figure 1, the Mountain View area is a pie-shaped wedge which has been rotated approximately 90° in a counter-clockwise direction and dipping to the northwest. The lowermost igneous unit, the Basal series, lies directly on the metasedimentary rocks and cannot be seen at this scale (fig. 1).

The rectangular area shown in figure 2 represents the drill-hole grid and is the copper and nickel exploration target in the Mountain View area of the Stillwater Complex. Due to the faulting and structural complexity of the region, only that part of this exploration area which is southwest of the Verdigris fault could be found to exhibit lithologic and structural continuity. This area, hereafter called the Mountain View study area, contains fault-bounded blocks that have been penetrated by enough drill holes (fig. 3) to credibly examine the lithologic and structural continuity of the mineralization.

Previously, the Stillwater Complex and adjacent rocks have been evaluated with respect to resources of nickel, copper, platinum-group metals, chromite, iron, aluminum, coal, and industrial rocks and minerals such as limestone, sand, and gravel (Page and Dohrenwend, 1973). That preliminary study was done at a very large scale and was

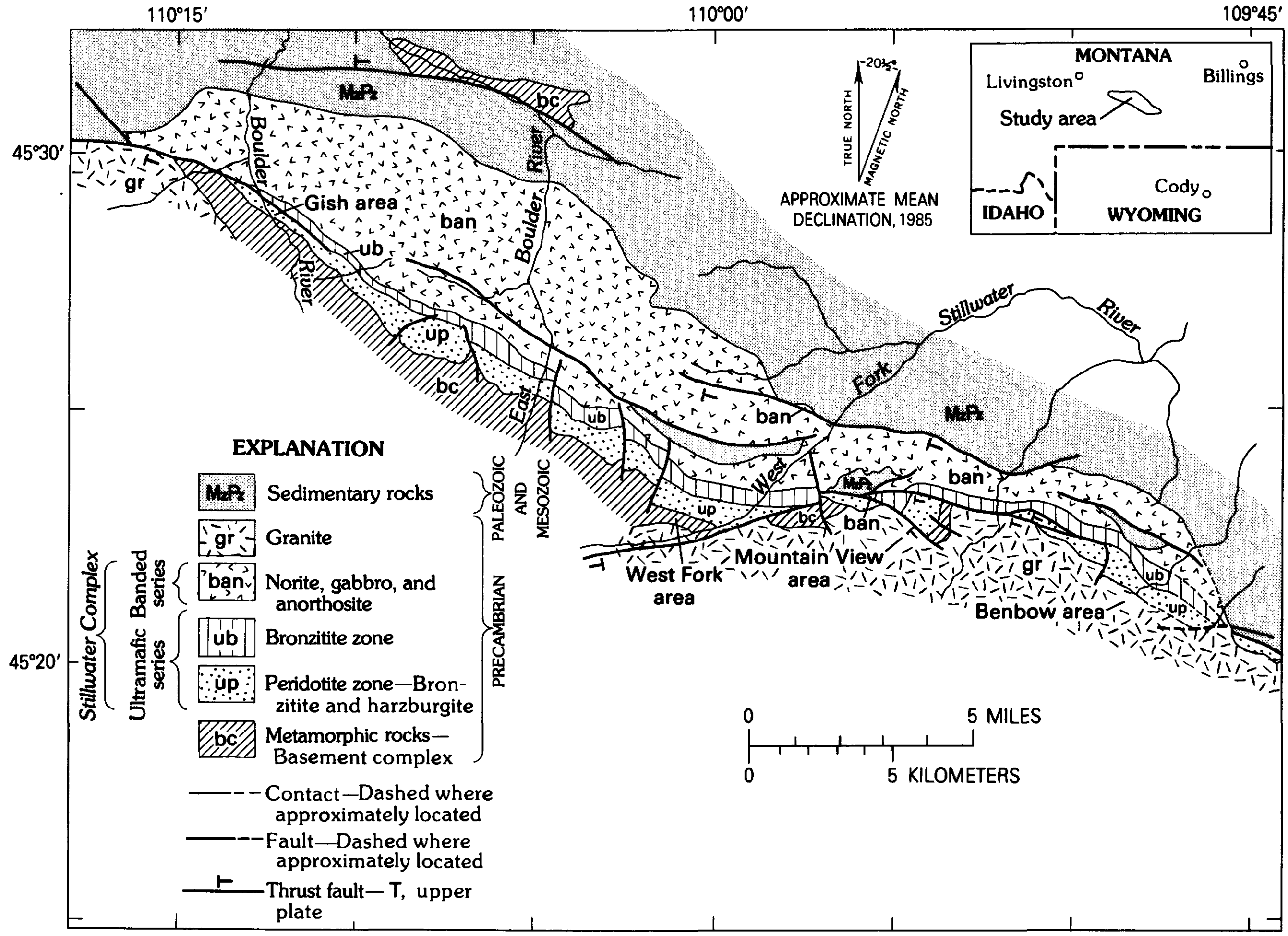

Figure 1. Geologic index map of the Stillwater Complex. Stratigraphic classification (Zientek, 1985) modified from Jackson (1961).

based on production and reserves of known mines and on prospects, mining company exploration, and geologic mapping and information. Our study deals with a much smaller part of the Stillwater Complex in greater detail and deals only with copper and nickel sulfides. The types of information incorporated into the analysis include data on copper and nickel concentrations as well as lithologic information from drill holes, previously mapped surficial geology, and computer-generated structural interpretation within the Mountain View study area.

The data on copper and nickel concentrations were evaluated in several different ways. First, statistics were computed using drill-hole concentration data within 100-foot horizontal intervals across the inclined stratigraphy of the study area southwest of the Verdigris fault. The resulting grade estimates were lower than those for currently operating underground copper and nickel mines.

The copper and nickel concentration data were analyzed within individual fault-bounded blocks and examined in 25-foot intervals both above and below the Basal series-metasedimentary rock contact and conformable to it. This analysis focused on the relation between the grades of copper and nickel and the distance from the Basal series-metasedimentary rock contact. We found that copper and nickel grades tend to decline as distance above and below this lithologic contact increases. The results also demonstrate the locations of rocks of potentially commercial grades in two of the fault-bounded blocks.

Only two fault-bounded blocks contained enough data to allow estimation of grade-tonnage relationships of in situ material. The fault block immediately west of the Verdigris fault (block VIII, fig. 3) contains approximately 17 to 22 million short tons of ore having an average grade of 0.5 percent combined copper and nickel. In the other fault-bounded block evaluated (block IV, fig. 3) which is located southwest of the first block, estimated tonnage is approximately 2 to 5 million short tons of ore, also having an average grade of 0.5 percent combined copper and nickel. Estimates are of in situ materials and do not allow for potential losses in mining, metallurgical recovery, and

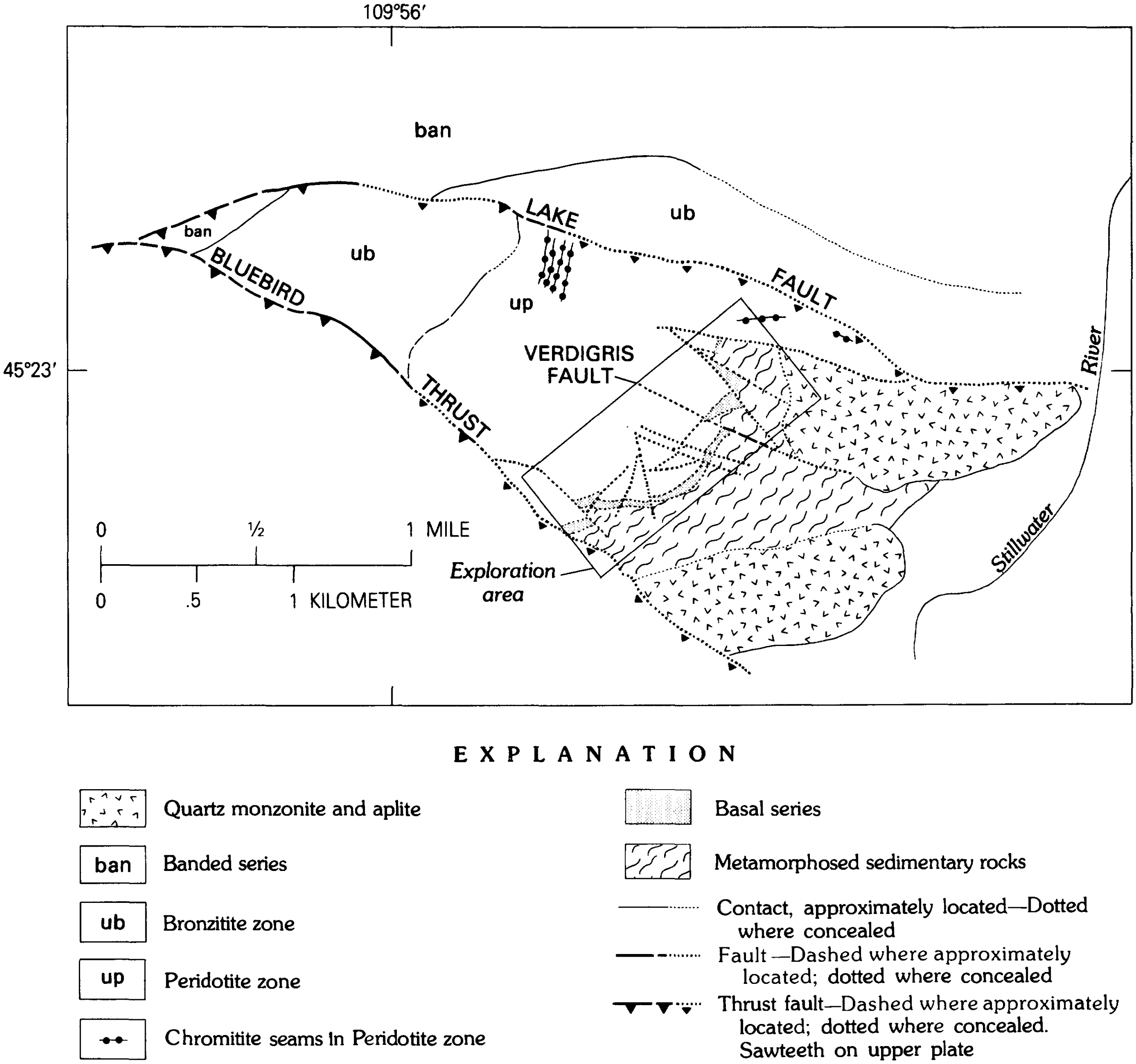

Figure 2. Generalized geologic index map of the Mountain View area (modified from Zientek, 1983).

losses due to the design of mines. These tonnages and grade estimates are uncertain because they are based on relatively sparse data. Additional sampling would be required in order to reduce this uncertainty. Future drilling should be focused on defining the continuity of mineralization within fault-bounded blocks in lithologic units lying above and below the contact between the Basal series and metasedimentary rocks.

This report first presents a general description of the geology. The distribution of metals by stratigraphic unit within the Mountain View study area is described. Then, concentration values within fault-bounded blocks in 25-foot intervals above and below the Basal series-metasedimentary rock contact are discussed. After that, the definition of potential mining units and the construction of grade-tonnage relationships is described along with the results of the analysis of concentration values. The concluding section summarizes the implications of the results in terms of siting future drill holes.

Acknowledgments

The authors wish to express their deepest gratitude to Anaconda Minerals Company for access to their exploration data and to Dr. Roger Cooper and Dr. Allistar

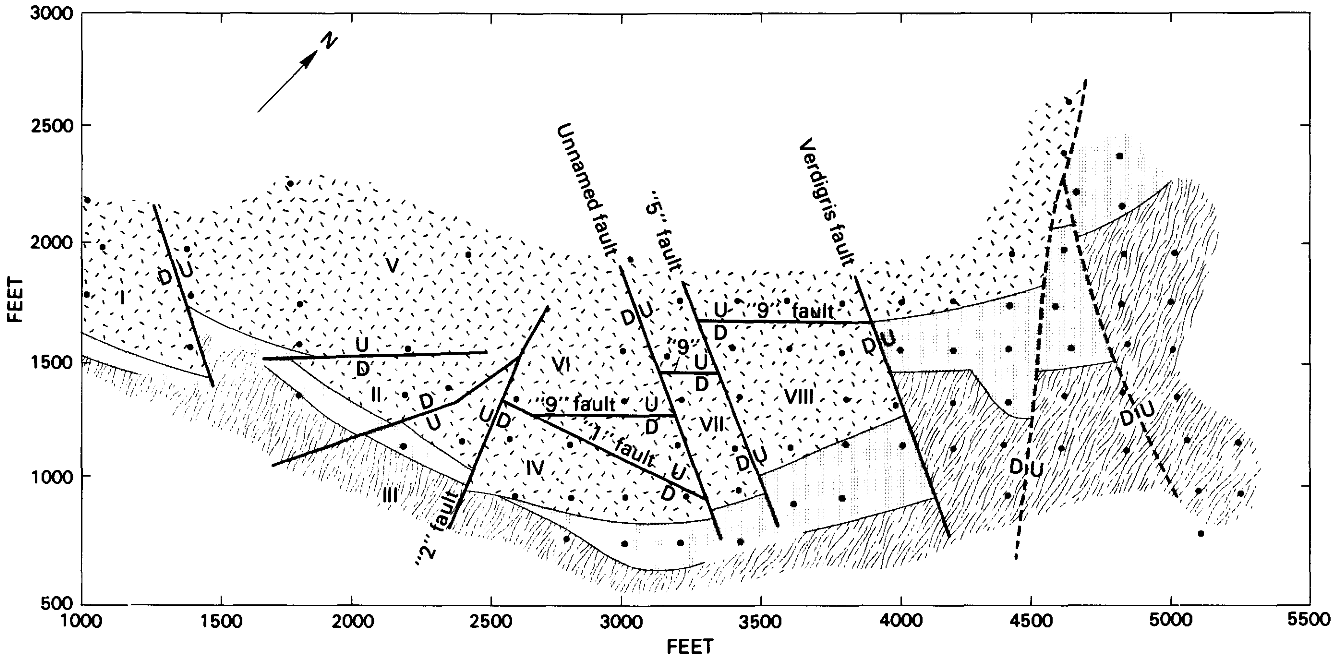

EXPLANATION

I—VIII Fault-bounded block numbers

U/D (solid line) Probable fault—Assumed vertical
U, Upthrown side
D, Downthrown side

U/D (dashed line) Probable fault—Not used in study
U, Upthrown side
D, Downthrown side

"1" fault Labeled faults referred to in text

BLOCK ORIENTATIONS

Block	Strike	Dip
I	N. 77°W.	35 NE
II	N. 75°E.	74 NW
III	N. 75°E.	74 NW
IV	N. 72°E.	49 NW
V	N. 82°E.	35 NW
VI	N. 76°E.	54 NW
VII	N. 68°E.	61 NW
VIII	N. 50°E.	65 NW

Ultramafic series

Basal series

Metasedimentary rocks

• Drill hole

—— Inferred contact

Figure 3. Base map showing drill-hole locations, faults, and fault-bounded block names, Mountain View area. Generalized geologic map modified from Zientek, 1983. Block orientation modified from Zientek, 1985, unpublished data. Scale is in feet.

Turner, without whose help this study would not have been possible. We would like to thank Dr. Norman J Page and Dr. Michael L. Zientek of the U.S. Geological Survey for their time and patience in familiarizing us with the geology of the area and for all the previous work done by them, upon which much of this study is based. The authors assume all responsibility for the generalized structural interpretation of the Mountain View area as presented in this study. Technical reviewers were Dr. John H. DeYoung, Jr., of the U.S. Geological Survey and Dr. John H. Schuenemeyer of the University of Delaware, whose critical comments helped to improve this paper.

GEOLOGIC SETTING

The Stillwater Complex is a large tabular mass of layered Late Archean mafic and ultramafic rocks and is exposed along the northern border of the Beartooth Mountains in southwestern Montana (fig. 1). It is approximately 30 miles (48 kilometers) long and has a maximum exposed thickness of 18,000 feet (5.5 kilometers)(Jackson, 1961). The layering in the complex strikes northwest and dips northeast. As the Stillwater Complex is only partly exposed and its upper units are eroded, its original size and shape are unknown.

The downward sequence of stratigraphic units contained within the Stillwater complex is shown in figure 4. Because drill holes used in this study are collared no higher than the Peridotite zone of the Ultramafic series, this is the highest stratigraphic unit included in this study. The Peridotite zone of the Ultramafic series, which commonly consists of cyclic repetitions of the cumulus sequence of olivine, olivine+ bronzite, and bronzite cumulates, is considered to conformably overlie the Basal series (Jackson, 1961; Page, 1977; Zientek and others, 1985). The Basal series, which has been subdivided into the Basal bronzite cumulate zone and the Basal norite zone

(Page and Nokleberg, 1974), is considered in this study to be one continuous cumulate unit consisting of bronzite cumulates above and a variety of cumulus minerals (olivine, orthopyroxene, clinopyroxene, plagioclase, and so on) plus sulfides near the bottom. Metasedimentary rocks of two types are present: cordierite-rich metasedimentary rocks, which are found in close proximity to the Basal series contact, and quartz-rich metasedimentary rocks, which are the dominant metasedimentary rock type and are infolded with the cordierite-rich facies (Zientek, 1983). An interval of sills and dikes associated with the Stillwater Complex and found only in the cordierite-rich metasedimentary rocks is contained within approximately 650 feet (200 meters)of the Basal series and is defined by the occurrence of diabase sills and dikes, mafic norite sills and dikes, and massive sulfides (Zientek, 1983).

The Mountain View area is a triangle-shaped area bounded by two high-angle reverse faults, the Lake fault and the Bluebird thrust (figs. 1, 2). As a consequence of rotation of this fault-bounded area, the stratigraphy strikes northeast and dips northwest. The rectangular area (fig. 2) is defined by a grid over which 110 drill holes are located. Eighty-six of these drill holes are vertical and used in the structural interpretation as presented here (fig. 3). The stratigraphy and fault intersections identified within each drill hole (used in conjunction with and constrained by the previously mapped surficial geology) resulted in a three-dimensional conceptual representation of the Mountain View study area. The structure, as presented here, is based on currently available data and is meant to serve as a framework from which grade-tonnage calculations can be computed. A more detailed geologic and structural interpretation of the area describing stratigraphy, morphology, and genesis of the units involved is the subject of another study.

The pattern of surface exposure of stratigraphic units for the structural interpretation used here is shown in figure 3. Shown within this figure are fault-bounded blocks, assumed vertical faults, vertical drill holes, and generalized surface stratigraphy.

Major northwest-trending faults appear to be the youngest and show left-lateral strike-slip movement. As a consequence of the faulting and the northwest dip of the stratigraphy, the area northeast of the Verdigris fault is dominantly metasedimentary rocks that have no known distribution or control on the contained sulfides. Orientations of the igneous rocks south and west of the Verdigris fault, however, can be determined from the layering of the cumulate rocks. The orientation for each fault-bounded block was computed from the lithologic contact between the Ultramafic series and the Basal series, which was assumed to be horizontal at the time of emplacement.

The distribution of sulfides within the Mountain View area is currently attributable to at least two processes: injection of sulfide-enriched mafic norites as dikes and sills into the cordierite-rich metasedimentary rocks (Zientek, 1983), and the coalescing and downward migration of immiscible sulfides through gravitational segregation during crystallization of the cumulate section (Page, 1979). The occurrence of sulfide-enriched sills and dikes with adjacent massive sulfides and the increase in sulfides toward the base of the Basal series have been observed and documented. Evidence is cited from both Zientek (1983) and Page (1979) to support the occurrence of these two events. The combination of these processes accounts for the concentration of sulfides in the proximity of the contact between the base of the Basal series and the metasedimentary rocks.

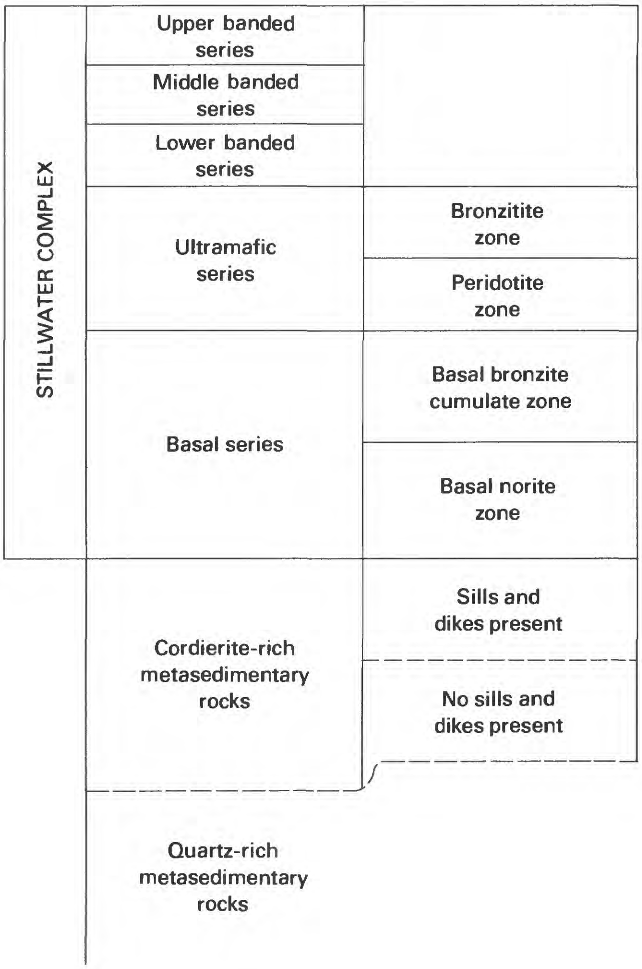

Figure 4. Stratigraphic classification of the Banded series, Ultramafic series, Basal series, and metasedimentary rocks used in this report (modified from Zientek, 1985). Illustration is not to scale.

DISTRIBUTION OF COPPER AND NICKEL BY STRATIGRAPHIC UNIT

Tables 1–5 show copper and nickel grades for the Peridotite zone of the Ultramafic series, Basal series,

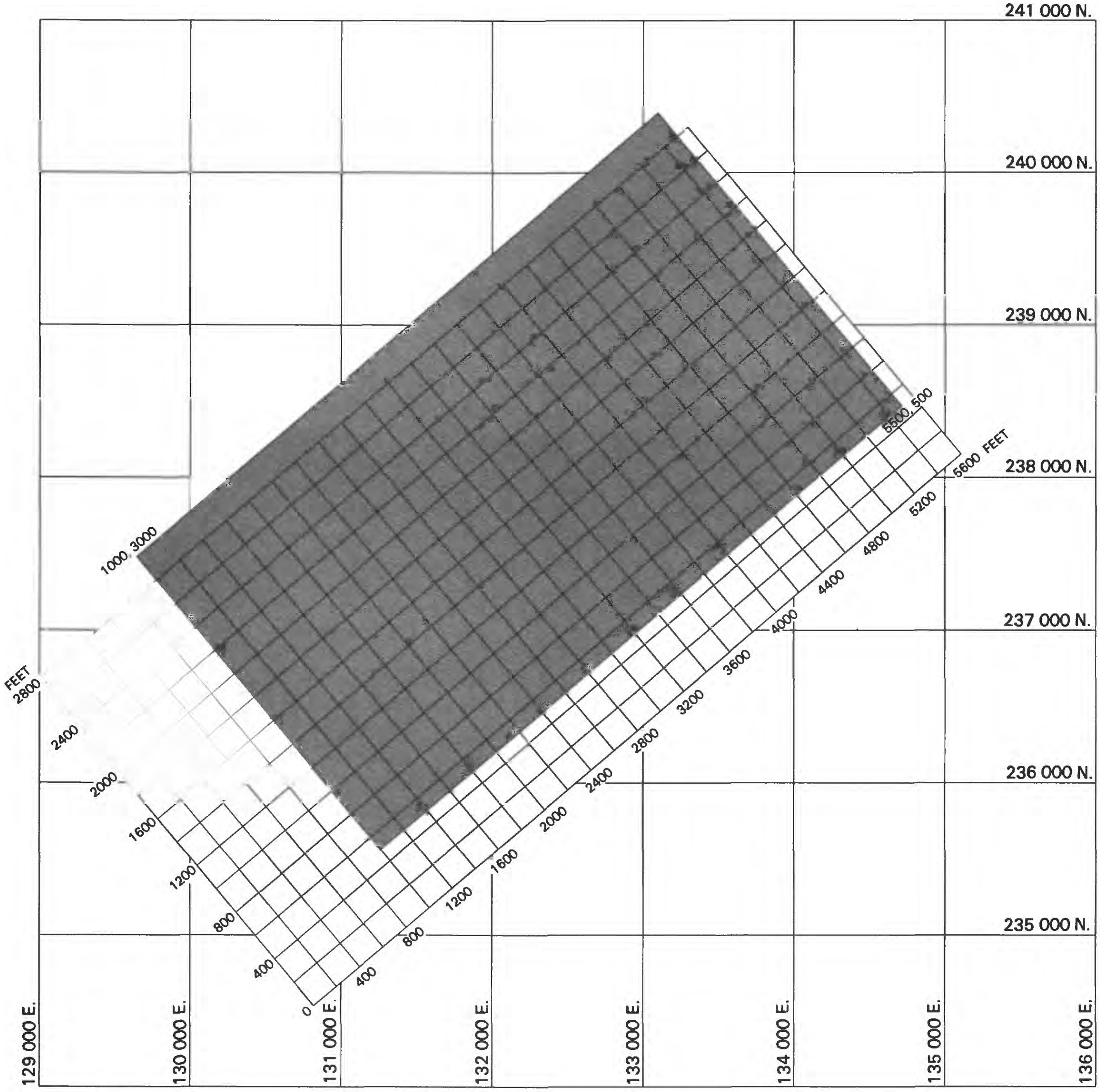

The coordinate system of figure 3 and subsequent figures is based on a gridded drilling program (above) developed by Anaconda Minerals Company to locate and space drill holes as accurately as possible for the Mouat prospect. The long dimension of this grid is oriented parallel to the strike of the stratigraphy and has drill holes located as closely as possible to 200-foot centers. The Anaconda grid is superimposed on a 10,000-meter Universal Transverse Mercator grid, zone 12 (1927 North American datum).

cordierite-rich metasedimentary rocks, quartz-rich metasedimentary rocks, and the sill- and dike-intruded metasedimentary rocks that have been delineated in the Mountain View study area of the Stillwater Complex (fig. 4). Only 46 of the 86 vertical drill holes used in the structural interpretation penetrated the Basal series and (or) the cordierite-rich metasedimentary rocks within the Mountain View study area southwest of the Verdigris fault. They are used in computing the stratigraphic unit statistics for the 100-foot horizontal intervals. All drill holes were continuously sampled and analyzed for copper and nickel metal concentrations. These values were derived from whole-rock analysis with an average sampling interval of approximately 6 feet. Because the analysis of copper and nickel came from whole rock samples, no distinction was made between metals incorporated in sulfide or silicate matrix. However, the amount of copper or nickel tied up as a silicate is very small whenever sulfide is also present in the sample. Although the Peridotite zone of the Ultramafic series and the quartz-rich metasedimentary rocks are not considered to contain the primary mining targets, grade statistics were computed for those sections that were contiguous to the Basal series or the cordierite-rich metasedimentary rocks.

All drill holes were calibrated to sea level, and the down-hole lithologic contacts were assigned vertical elevations above sea level. Data were examined in 100-foot horizontal intervals across the study area southwest of the Verdigris fault. An idealized cross section for the 6,700- to 6,800-foot interval used in tables 1–5 is illustrated in figure 5. Within each stratigraphic unit and 100-foot horizontal interval above sea level, all well logs were searched for the corresponding copper and nickel concentration values. For concentration data from a drill hole to be included in the computations for a particular 100-foot interval, the drill hole must have penetrated at least half of that interval. For each drill hole that met the conditions of correct 100-foot interval and stratigraphic unit, the concentration values were tabulated corresponding to the individual vertical elevation intervals for each hole, and an average grade weighted by length of each sample was computed. A drill hole is then represented in each 100-foot interval by a point corresponding to the down-hole weighted average of concentration measurements. Figure 5 is an idealized cross section for the 6,750-foot-midpoint interval. In reality, the nine holes penetrating the 6,700- to 6,800-foot interval of the Peridotite zone of the Ultramafic series (table 1), six holes penetrating the 6,700- to 6,800-foot interval of the Basal series (table 2), and so on, are distributed among eight fault-bounded blocks in the part of the study area west of the Verdigris fault. Thus, the drill holes sample different fault-bounded blocks and different stratigraphic elevations above the base of the units involved.

The first column in tables 1–5 gives the elevation of the midpoints of the 100-foot intervals examined. The second column indicates the number of holes that penetrated each 100-foot interval. The next five columns give the means and standard deviations of the copper and nickel grades and the corresponding correlation coefficients for copper and nickel grades. The columns in the remainder of the table provide additional information about the distribution of concentration values in the form of the 50th percentile value (median), 75th percentile value, and maximum concentration value for a sample occurring in each 100-foot interval.

Table 1 shows statistics computed from concentration data for 100-foot intervals of drill holes in the Peridotite zone of the Ultramafic series. The mean copper grades are usually less than half the mean nickel grades. Nickel is dominantly present as a silicate, occurring within the crystal silicate structure of the olivines. However, there is also nickel present in the very minor occurrences of sulfide minerals pentlandite and pyrrhotite within the Ultramafic series. Copper is dominantly present in the sulfide mineral chalcopyrite. The results show that the median copper grades are consistently smaller than the mean copper grade, implying that in each data set the mean is influenced by large copper grade values. The correlation coefficient between copper and nickel is always positive, but none of the values were significant at the 99-percent confidence level.

Similar statistics for the Basal series are shown in table 2. Copper grades and nickel grades are substantially higher here than in the Peridotite zone. Both copper and nickel are present dominantly in sulfide form; copper is present in chalcopyrite and nickel in pentlandite and pyrrhotite. For each midpoint in table 2, correlations between cooper and nickel are considerably higher than the correlations observed within the Peridotite zone (table 1). The mean copper grades are still larger than the median grades, indicating a skewed distribution of grades within each 100-foot interval. There was only one midpoint, at 5,350 feet, where the combined mean copper and nickel grades are greater than 0.5 percent. Other intervals, where the sum of the mean copper grade and the mean nickel grade exceeds 0.4 percent, are from 6,050 to 5,950 feet and from 5,550 to 5,050 feet, respectively.

Table 3 shows results for the cordierite-rich metasedimentary rocks, including unintruded areas and areas intruded by sills and dikes. Only four of the 100-foot intervals have combined mean copper and nickel grades of more than 0.4 percent. These midpoints are located in the interval from 5,550 to 5,250 feet. Copper and nickel are also predominately in their sulfide forms here. Statistics for the quartz-rich metasedimentary rocks are presented in table 4; both the mean (and even maximum) copper and nickel grades are very low.

The stratigraphy of the cordierite-rich metasedimentary rocks was further refined into intruded metasedimentary rock, representing a sill and dike association of border rocks, and unintruded metasediments (fig. 4). Of the 46 original drill holes located southwest of the Verdigris fault which penetrated either the Basal series or cordierite-rich metasedimentary rocks, only 23 contained sills and dikes which are presumed to be associated with the Stillwater intrusion. Grade statistics for the intruded metasedimentary rocks, table 5, generally show higher copper and nickel concentrations than the combined unintruded and intruded cordierite-rich metasedimentary rocks (table 3).

Grades presented in tables 2, 3, and 5, where copper and nickel are predominately in sulfide forms, represent a sampling of these units within the Mountain View study area. These grades are lower than those for currently

Table 1. Statistics computed from drill-hole data on copper and nickel concentrations in the Peridotite zone of the Ultramafic series of the Mountain View study area, Stillwater Complex

[Grades are in weight percent; ---, no data]

Midpoint of 100-ft interval	No. of holes	Mean copper grade	Standard deviation, copper grade	Mean nickel grade	Standard deviation, nickel grade	Correlation copper vs. nickel grade[1]	50 percentile		75 percentile		Maximum values	
							Copper grade	Nickel grade	Copper grade	Nickel grade	Copper grade	Nickel grade
7050------	4	0.038	0.021	0.120	0.061	0.5073	0.023	0.097	0.052	0.106	0.060	0.210
6950------	9	.038	.025	.086	.062	.5954	.030	.080	.040	.096	.080	.230
6850------	9	.051	.034	.091	.024	.2488	.040	.087	.062	.109	.120	.120
6750------	9	.058	.046	.107	.051	.6585	.035	.099	.079	.124	.150	.200
6650------	15	.055	.050	.098	.052	.4041	.047	.090	.063	.125	.220	.210
6550------	19	.042	.026	.116	.056	.1076	.029	.111	.048	.155	.110	.220
6450------	23	.054	.031	.146	.072	.4823	.048	.155	.065	.174	.120	.370
6350------	16	.048	.019	.146	.050	.1395	.041	.157	.052	.177	.100	.250
6250------	14	.046	.027	.142	.070	.1570	.030	.141	.049	.175	.100	.210
6150------	12	.039	.020	.130	.047	.5179	.030	.126	.050	.163	.070	.210
6050------	10	.050	.028	.174	.040	.4247	.031	.165	.068	.189	.100	.260
5950------	10	.038	.027	.160	.047	.7537	.031	.138	.047	.168	.090	.280
5850------	3	.040	.010	.143	.010	.1555	---	---	---	---	.050	.180

[1]None of the correlations are significant at 99-percent confidence level.

Table 2. Statistics computed from drill-hole data on copper and nickel concentrations in the Basal series of the Mountain View study area, Stillwater Complex

[Grades are in weight percent; ---, no data]

Midpoint of 100-ft interval	No. of holes	Mean copper grade	Standard deviation, copper grade	Mean nickel grade	Standard deviation, nickel grade	Correlation copper vs. nickel grade	50 percentile		75 percentile		Maximum values	
							Copper grade	Nickel grade	Copper grade	Nickel grade	Copper grade	Nickel grade
6850------	1	0.090	---	0.130	---	---	---	---	---	---	---	---
6750------	6	.142	0.059	.177	0.057	0.7560	0.115	0.183	0.149	0.206	0.240	0.220
6650------	9	.123	.105	.129	.078	.7664	.077	.113	.185	.183	.320	.260
6550------	11	.118	.063	.142	.104	[1].8676	.102	.120	.132	.170	.270	.410
6450------	16	.134	.057	.135	.048	.4746	.123	.123	.162	.166	.270	.230
6350------	21	.160	.091	.183	.080	[1].7646	.139	.185	.227	.244	.400	.330
6250------	17	.158	.059	.186	.074	.5731	.147	.196	.200	.224	.280	.360
6150------	11	.140	.059	.175	.092	[1].8199	.130	.165	.170	.213	.260	.330
6050------	10	.233	.099	.251	.130	.6396	.218	.210	.280	.336	.440	.490
5950------	6	.205	.091	.200	.109	[1].9333	.193	.147	.235	.222	.360	.390
5850------	11	.125	.071	.128	.061	[1].8460	.108	.127	.152	.166	.260	.200
5750------	10	.148	.068	.143	.066	[1].8008	.134	.135	.200	.192	.230	.230
5650------	11	.184	.150	.175	.113	[1].9690	.156	.166	.233	.215	.570	.460
5550------	7	.220	.124	.271	.093	.8141	.181	.260	.226	.325	.460	.420
5450------	5	.190	.107	.254	.166	.9347	.142	.181	.254	.378	.350	.440
5350------	5	.318	.202	.362	.341	.8595	.253	.222	.378	.331	.620	.960
5250------	3	.222	.042	.210	.121	.2774	---	---	---	---	.270	.280
5150------	1	.220	---	.220	---	---	---	---	---	---	---	---
5050------	1	.160	---	.250	---	---	---	---	---	---	---	---
4950------	1	.130	---	.180	---	---	---	---	---	---	---	---

[1]Correlations are significant at 99-percent confidence level.

Table 3. Statistics computed from drill-hole data on copper and nickel concentrations in the cordierite-rich metasedimentary rocks of the Mountain View study area, Stillwater Complex

[Grades are in weight percent; ---, no data]

Midpoint of 100-ft interval	No. of holes	Mean copper grade	Standard deviation, copper grade	Mean nickel grade	Standard deviation, nickel grade	Correlation copper vs. nickel grade	50 percentile		75 percentile		Maximum values	
							Copper grade	Nickel grade	Copper grade	Nickel grade	Copper grade	Nickel grade
6850------	1	0.110	---	0.060	---	---	---	---	---	---	---	---
6750------	3	.067	0.025	.083	0.021	0.7954	---	---	---	---	0.090	0.100
6650------	3	.107	.055	.103	.061	.9707	---	---	---	---	.160	.170
6550------	5	.156	.079	.162	.067	[1].9763	0.127	0.150	0.186	0.171	.270	.270
6450------	5	.152	.071	.144	.113	.9419	.129	.116	.206	.199	.230	.300
6350------	6	.165	.188	.123	.114	[1].9623	.063	.092	.180	.123	.530	.340
6250------	9	.131	.125	.143	.094	.7499	.087	.123	.167	.191	.420	.310
6150------	12	.133	.074	.136	.102	[1].8363	.132	.110	.193	.170	.289	.270
6050------	9	.138	.135	.081	.048	.5524	.069	.076	.150	.111	.420	.160
5950------	10	.163	.123	.170	.153	[1].7729	.121	.090	.251	.282	.370	.390
5850------	1	.140	---	.160	---	---	---	---	---	---	---	---
5750------	5	.090	.063	.116	.111	.9350	.070	.062	.088	.134	.200	.300
5650------	3	.113	.078	.103	.078	.9990	---	---	---	---	.200	.190
5550------	4	.233	.088	.293	.214	.1593	.183	.227	.360	.234	.360	.560
5450------	6	.227	.110	.178	.107	−0.0261	.197	.113	.265	.247	.410	.330
5350------	3	.263	.206	.180	.115	.4799	---	---	---	---	.480	.290
5250------	1	.250	---	.800	---	---	---	---	---	---	---	---
5150------	2	.065	---	.105	---	---	---	---	---	---	.120	.120
5050------	1	.010	---	.000	---	---	---	---	---	---	---	---
4950------	1	.020	---	.050	---	---	---	---	---	---	---	---

[1]Correlations are significant at 99-percent confidence level.

operating underground mines. As figure 5 shows, the concentration data analyzed by 100-foot elevation intervals result in a collection of summary statistics that includes samples from different elevation levels within each stratigraphic unit. Moreover, figure 3 shows that the area is composed of several fault-bounded blocks and that each block has a unique orientation. In an effort to identify the rock units with high grades and to estimate ore tonnages, the drill-hole concentration data will be examined on the basis of uniform stratigraphic heights within the lithologic unit both above and below the base of the Basal series.

DISTRIBUTION OF COPPER AND NICKEL ALONG THE BASAL SERIES-METASEDIMENTARY ROCK CONTACT

As a result of the combination of sulfide-enriched mafic norites intruding the cordierite-rich metasedimentary rocks (Zientek, 1983) and of sulfide immiscibility and gravitational settling within the Basal series cumulates (Page, 1979), the highest concentrations of copper and nickel sulfides are expected to be found directly above and below the contact between the Basal series and the metasedimentary rocks (Drew and others, 1985). Fault blocks constituting the Mountain View study area have been rotated, translated, and inclined due to faulting after the introduction of the copper and nickel sulfides. Hence, the stratigraphy now appears to be discontinuous when examined in horizontal intervals.

Another method by which to evaluate the distribution of copper and nickel sulfides is to examine the mean grades in 25-foot layers conformable to the Basal series and metasedimentary rock contact, both above into the Basal series and below into the metasedimentary rocks. The thickness of each 25-foot rock layer was measured perpendicular to the Ultramafic series-Basal series contact using block orientations as shown in figure 3. All drill-hole data, including copper-nickel concentrations and lithologies within each fault-bounded block, were recomputed to account for orientation of the block.

Results of these computations are presented in table 6 and in figure 6. B1 represents the 25-foot interval in the Basal series just above the contact, while C1 represents the 25-foot interval just beneath the contact but within the cordierite-rich metasedimentary rocks. B2 and C2 are layers above and below B1 and C1, respectively. Similarly, results for 175 to 200 feet above (B8) and 175 to 200 feet below (C8) the contact were computed and are displayed.

Table 4. Statistics computed from drill-hole data on copper and nickel concentrations in the quartz-rich metasedimentary rocks of the Mountain View study area, Stillwater Complex

[Grades are in weight percent; ---, no data]

Midpoint of 100-ft interval	No. of holes	Mean copper grade	Standard deviation, copper grade	Mean nickel grade	Standard deviation, nickel grade	Correlation copper vs. nickel grade[1]	50 percentile		75 percentile		Maximum values	
							Copper grade	Nickel grade	Copper grade	Nickel grade	Copper grade	Nickel grade
6750------	1	0.010	---	0.080	---	---	---	---	---	---	---	---
6650------	1	.020	---	.050	---	---	---	---	---	---	---	---
6550------	2	.040	---	.050	---	---	---	---	---	---	0.050	0.060
6450------	3	.033	0.023	.033	0.015	0.9449	---	---	---	---	.060	.050
6350------	5	.054	.011	.036	.023	.4572	0.048	0.038	0.059	0.050	.070	.060
6250------	7	.051	.041	.024	.022	.1028	.050	.070	.050	.035	.140	.060
6150------	5	.038	.013	.022	.016	−0.6768	.037	.016	.046	.029	.050	.040
6050------	6	.032	.024	.030	.028	.2278	.023	.021	.042	.037	.070	.080
5950------	1	.020	---	.030	---	---	---	---	---	---	---	---
5850------	3	.147	.193	.033	.006	.9997	---	---	---	---	.370	.040
5750------	1	.120	---	.020	---	---	---	---	---	---	---	---
5650------	2	.080	---	.015	---	---	---	---	---	---	.130	.020
5550------	2	.185	---	.240	---	---	---	---	---	---	.350	.430
5450------	1	.070	---	.100	---	---	---	---	---	---	---	---
5350------	1	.020	---	.040	---	---	---	---	---	---	---	---
5250------	1	.020	---	.060	---	---	---	---	---	---	---	---
5150------	0	---	---	---	---	---	---	---	---	---	---	---
5050------	0	---	---	---	---	---	---	---	---	---	---	---
4950------	1	.010	---	.050	---	---	---	---	---	---	---	---
4850------	1	.010	---	.000	---	---	---	---	---	---	---	---

[1]None of the correlations are significant at 99-percent confidence level.

Table 5. Statistics computed from drill-hole data on copper and nickel concentrations in the sill- and dike-intruded metasedimentary rocks of the Mountain View study area, Stillwater Complex

[Grades are in weight percent; ---, no data]

Midpoint of 100-ft interval	No. of holes	Mean copper grade	Standard deviation, copper grade	Mean nickel grade	Standard deviation, nickel grade	Correlation copper vs. nickel grade	50 percentile		75 percentile		Maximum values	
							Copper grade	Nickel grade	Copper grade	Nickel grade	Copper grade	Nickel grade
6750------	2	0.080	---	0.095	---	---	---	---	---	---	0.090	0.100
6650------	3	.110	0.055	.103	0.061	0.970	0.087	0.078	0.129	0.118	.160	.170
6550------	5	.156	.079	.162	.067	[1].980	.127	.150	.186	.171	.270	.270
6450------	5	.152	.079	.144	.113	.940	.129	.116	.206	.199	.230	.300
6350------	3	.283	.216	.197	.124	.980	.183	.130	.300	.190	.530	.340
6250------	6	.163	.138	.167	.101	.700	.141	.142	.192	.226	.420	.310
6150------	8	.174	.053	.181	.094	.680	.142	.137	.206	.275	.270	.310
6050------	6	.187	.143	.092	.056	.470	.124	.104	.316	.154	.420	.160
5950------	7	.233	.134	.230	.142	.620	.230	.213	.293	.342	.430	.410
5850------	1	.140	---	.060	---	---	---	---	---	---	---	---
5750------	1	.200	---	.300	---	---	---	---	---	---	---	---
5650------	1	.050	---	.040	---	---	---	---	---	---	---	---
5550------	3	.190	.026	.273	.026	−0.060	.178	.160	.199	.373	.220	.560
5450------	5	.212	.116	.148	.086	−0.370	.178	.100	.212	.177	.410	.280
5350------	3	.263	.206	.180	.115	.480	.179	.137	.322	.225	.480	.290
5250------	1	.250	---	.800	---	---	---	---	---	---	---	---
5150------	1	.120	---	.210	---	---	---	---	---	---	---	---

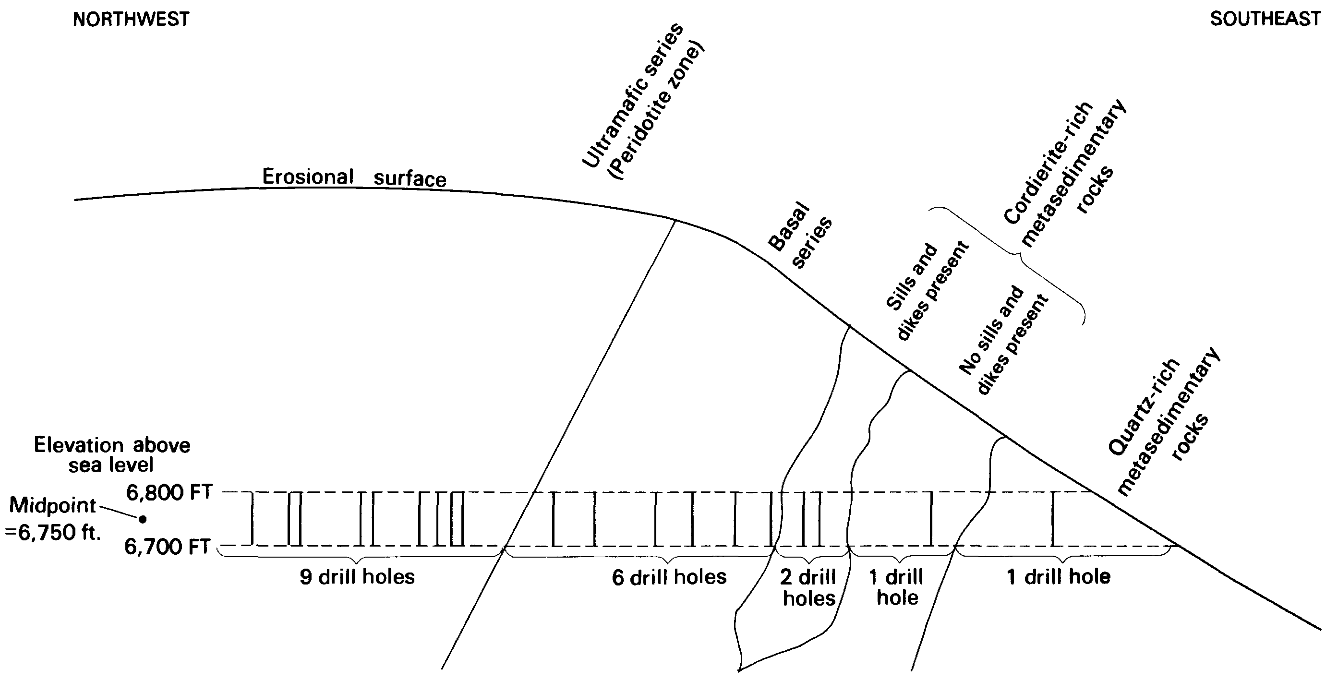

Figure 5. Idealized cross section (perpendicular to strike) of the 6,750-foot midpoint interval demonstrating the method used to compute statistics for 100-foot horizontal intervals represented in tables 1–5. Stratigraphy dipping approximately 60° to the northwest.

Results generally support the hypothesis that within the Basal series higher concentrations of copper and nickel sulfides are found closer to the Basal series-metasedimentary rock contact (Page, 1979). Copper and nickel grades tend to decrease with an increase in distance both above and below the contact. There may be some distortion to the copper and nickel grades assigned to true stratigraphic position because of faults which were encountered within these distances from the contact. However, in most cases the distortions are not thought to be consistent from block to block or drill hole to drill hole and, hence, do not constitute a systematic change within the patterns.

Table 6 shows the average copper and nickel grades in 25-foot intervals measured away from the Basal series-metasedimentary rock contact by fault-bounded block. Also shown is the percentage of footage having combined copper and nickel grades of at least 0.5 percent for each interval. This column, along with the average grades, shows whether high grade levels are the result of a few feet of anomalously high core measurements or whether they are typical of the entire interval of core.

From table 6 it can be shown that the combined mean copper and mean nickel grades exceed 0.5 percent in only 11 of 111 25-foot intervals across all eight fault-bounded blocks for which data are available. Furthermore, in only two of the eleven 25-foot intervals having combined average grades above 0.5 percent does at least half of the core assayed exceed that cutoff value (block V, interval B1, and block VIII, interval C6). Even though combined mean copper and nickel grades for most of the intervals shown do not exceed 0.5 percent, each will generally have some core footage, usually greater than 5 percent of the total footage assayed, where the combined copper and nickel grade values exceed 0.5 percent.

Blocks I, IV, and VI have no 25-foot intervals with combined average copper and nickel grades above 0.5 percent (table 6). Block V has three 25-foot intervals (B1, C1, and C8) with average combined grades above 0.5 percent. However, only the B1 and C1 layers in block V, which are penetrated by three drill holes each, have 40 percent or more of their measured core above the 0.5-percent combined grade level. In blocks III and VII, the intervals having average grades above the 0.5-percent combined grade level are penetrated by only one hole; therefore, the opportunities for geologic or statistical inference are very limited. Block VIII appears, by far, to be the most interesting in terms of identifying potentially minable sections. It contains three intervals having average grades above the combined 0.5-percent level (B1, C5, and C6), and it contains 16 holes in one of those intervals.

The distribution of copper and nickel in fault blocks IV and VIII is examined in more detail in the next section. These blocks have the largest number of holes penetrating the Basal series-metasedimentary rock contact, where one

Table 6. Average copper and nickel grades in 25-foot intervals measured away from the Basal series-metasedimentary rock contact by fault-bounded block

[Grade is in weight percent; ---, no data; cutoff=percent of true footage in 25-foot interval where sum of copper and nickel grades is greater or equal to 0.50 percent]

25-foot Interval	Block I				Block II				Block III				Block IV			
	No. of holes	Mean Cu grade	Mean Ni grade	Percent above cutoff	No. of holes	Mean Cu grade	Mean Ni grade	Percent above cutoff	No. of holes	Mean Cu grade	Mean Ni grade	Percent above cutoff	No. of holes	Mean Cu grade	Mean Ni grade	Percent above cutoff
B8 ---	2	0.16	0.13	7	---	---	---	---	---	---	---	---	4	0.06	0.06	6
B7 ---	2	.06	.07	0	1	0.04	0.04	0	---	---	---	---	5	.06	.04	2
B6 ---	2	.07	.03	5	1	.07	.04	0	---	---	---	---	6	.09	.11	1
B5 ---	2	.10	.14	0	1	.11	.09	0	---	---	---	---	7	.13	.17	6
B4 ---	3	.20	.25	24	1	.14	.14	0	---	---	---	---	7	.14	.17	12
B3 ---	3	.10	.12	0	1	.22	.22	19	---	---	---	---	8	.15	.19	14
B2 ---	3	.25	.15	14	2	.12	.15	15	---	---	---	---	9	.17	.18	15
B1 ---	4	.17	.19	20	2	.12	.13	5	1	0.07	0.07	0	9	.21	.23	32
*------																
C1 ---	4	.17	.22	26	3	.22	.29	9	1	.14	.12	15	9	.20	.24	37
C2 ---	4	.09	.13	18	3	.09	.10	7	1	.25	.25	46	7	.21	.22	25
C3 ---	3	.04	.03	0	3	.10	.07	6	1	.22	.23	21	6	.20	.14	22
C4 ---	1	.03	.06	0	2	.13	.13	9	1	.06	.04	6	5	.22	.22	19
C5 ---	1	.08	.08	0	3	.14	.14	9	---	---	---	---	2	.07	.04	5
C6 ---	1	.10	.09	0	2	.14	.02	4	---	---	---	---	2	.20	.05	17
C7 ---	---	---	---	---	1	.46	.12	44	---	---	---	---	1	.17	.05	11
C8 ---	---	---	---	---	1	.03	.03	0	---	---	---	---	1	.33	.06	15

25-foot Interval	Block V				Block VI				Block VII				Block VIII			
	No. of holes	Mean Cu grade	Mean Ni grade	Percent above cutoff	No. of holes	Mean Cu grade	Mean Ni grade	Percent above cutoff	No. of holes	Mean Cu grade	Mean Ni grade	Percent above cutoff	No. of holes	Mean Cu grade	Mean Ni grade	Percent above cutoff
B8 ---	2	0.19	0.14	24	1	0.13	0.17	8	1	0.13	0.17	8	8	0.17	0.16	25
B7 ---	2	.17	.17	18	2	.18	.18	12	1	.15	.20	0	10	.18	.20	20
B6 ---	2	.14	.13	2	2	.25	.21	57	1	.24	.31	43	12	.16	.19	10
B5 ---	2	.15	.10	0	2	.19	.20	18	1	.25	.29	49	12	.12	.16	11
B4 ---	2	.22	.15	8	2	.19	.16	16	2	.14	.16	13	12	.18	.09	22
B3 ---	2	.16	.15	0	3	.09	.08	0	2	.14	.21	23	13	.18	.25	31
B2 ---	2	.17	.19	9	3	.20	.16	11	3	.13	.16	9	16	.25	.17	35
B1 ---	3	.39	.46	64	3	.21	.24	29	3	.17	.24	21	16	.31	.32	49
*------																
C1 ---	3	.22	.29	41	3	.16	.29	21	4	.08	.15	8	10	.20	.27	28
C2 ---	3	.13	.17	23	3	.19	.13	15	3	.11	.12	11	7	.19	.09	18
C3 ---	3	.11	.17	15	3	.04	.05	1	3	.09	.14	7	4	.13	.19	27
C4 ---	3	.13	.19	25	3	.10	.10	11	3	.08	.11	9	3	.12	.13	18
C5 ---	3	.12	.11	14	2	.06	.04	5	2	.04	.05	0	2	.15	.43	43
C6 ---	2	.08	.06	0	1	.05	.02	0	2	.05	.05	0	1	.26	.64	85
C7 ---	2	.19	.27	39	---	---	---	---	2	.04	.06	0	1	.16	.27	19
C8 ---	2	.38	.13	16	---	---	---	---	2	.06	.13	10	---	---	---	---

*Dashed lines denote contact between Basal series and cordierite-rich metasedimentary rocks.

would expect to find the highest grades. But even in these blocks, the number of holes was insufficient to use anything but the most elementary engineering methods for resource evaluation. Substantial additional drilling is necessary in order to further refine the subsurface of these blocks or of other fault-bounded blocks.

IN SITU GRADE-TONNAGE RELATIONS FOR FAULT BLOCKS IV AND VIII

Previous sections of this paper described copper-nickel concentration values in various degrees of detail. The concentration values of copper and nickel in horizon-

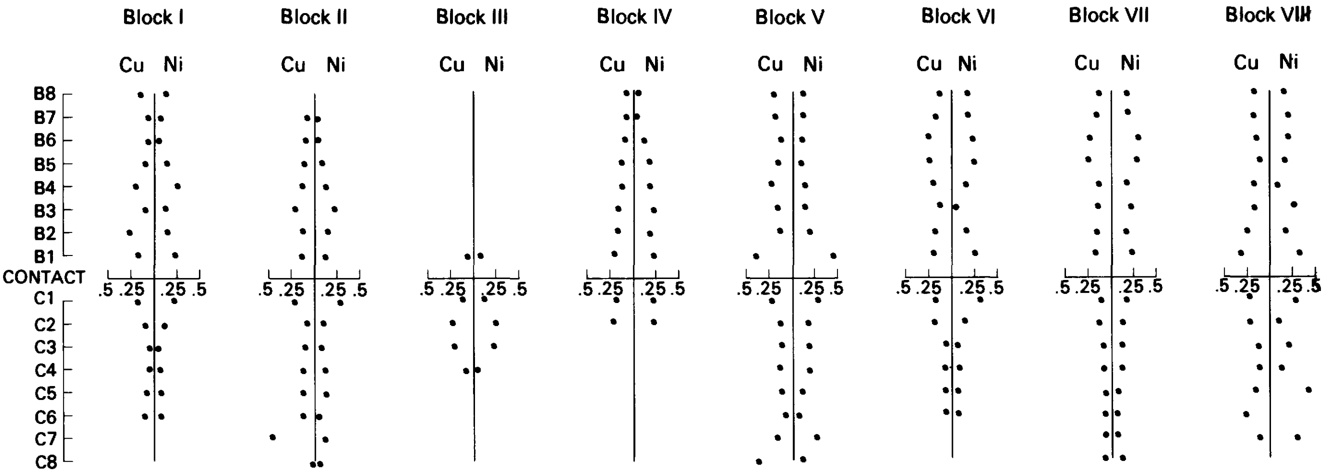

Figure 6. Distribution of copper and nickel by 25-foot intervals away from the Basal series-metasedimentary rock contact within individual fault-bounded blocks. Grades are in weight percent. Intervals B1 through B8 represent successive 25-foot rock layers above the Basal series-metasedimentary rock contact, and intervals C1 through C8 represent 25-foot rock layers below this contact.

tal 100-foot intervals by stratigraphic unit in drill holes of the Mountain View study area were already described. Copper-nickel concentration values for 25-foot intervals above and below the Basal series-metasedimentary rock contact were then examined within individual fault blocks.

In this section, a further refinement of the analysis of concentration values is made, and results of the in situ ore tonnage calculations of blocks IV and VIII are presented. The areal extent of each 25-foot layer was delineated according to the structural interpretation of the subsurface geology derived from drill-hole information and surficial geology. Continuity of 25-foot intervals, both above and below the base of the Basal series, was correlated as far as possible. Lateral continuity, however, has been affected between blocks by faulting, rotation, and translation of the fault-bounded blocks; within blocks by erosional truncation and the natural variability of thickness resulting in pinching of the beds; and by loss of control due to the inclined stratigraphy and the lack of drill-hole information.

We assume that mining units within individual fault-bounded blocks would be along the lower Basal series contact. The mineralization and stratigraphy are assumed to be continuous along the contact between the Basal series and cordierite-rich metasedimentary rocks where it could not be shown otherwise. Intervals of 25 feet, which are conformable to the contact and spatially limited by the structural interpretation, were examined both upward into the cumulate rocks of the Basal series and downward from the contact into the metasedimentary rocks. The area of the contact for each block (fig. 3) was measured at the surface by planimeter and adjusted to account for the inclination of the stratigraphy.

Block VIII is penetrated by 14 vertical drill holes which are used in the structural interpretation of this block (fig. 3). Additionally, two angle holes were incorporated to compute the grade-tonnage statistics for this block. Block VIII is delineated by (1) an assumed vertical Verdigris fault in the northeast; (2) an assumed vertical number "5" fault in the southwest; (3) erosional truncation due to inclination of the Basal series-metasedimentary rock contact in the southeast; and (4) a vertical boundary positioned by loss of control due to the lack of holes and increasing depth of the body to the northwest. Two subfaults, which are approximately parallel and supplementary to the Verdigris fault (V2 and V3), are positioned as interpreted to be located at the base of the Basal series and assumed to be vertical for calculations. In reality, they are interpreted to be dipping at approximately 70° to the southwest. At depth, this area becomes 1,475,000 square feet due to the 65° angle of inclination.

The orientation of block VIII, based on the Ultramafic series-Basal series contact, is N. 50° E., 65° NW. This orientation results from the surficial geology, the evidence for minor faulting within this block, and a combination of multiple three-point problems computed on drill holes that penetrate the Ultramafic series-Basal series contact. This is the best orientation that can be interpreted from currently available information. A computer-generated elevation contour map of the base of the Basal series for block VIII is shown in figure 7 which can be oriented to figure 3 by means of the horizontal and vertical scales. The Basal series-metasedimentary rock contact dips northwest at a high angle from 6,300 feet above sea level until the number "9" fault is encountered at 5,250 feet. Here the contour appears flat because the northwest side of the number "9" fault has moved the lower Basal series contact upward.

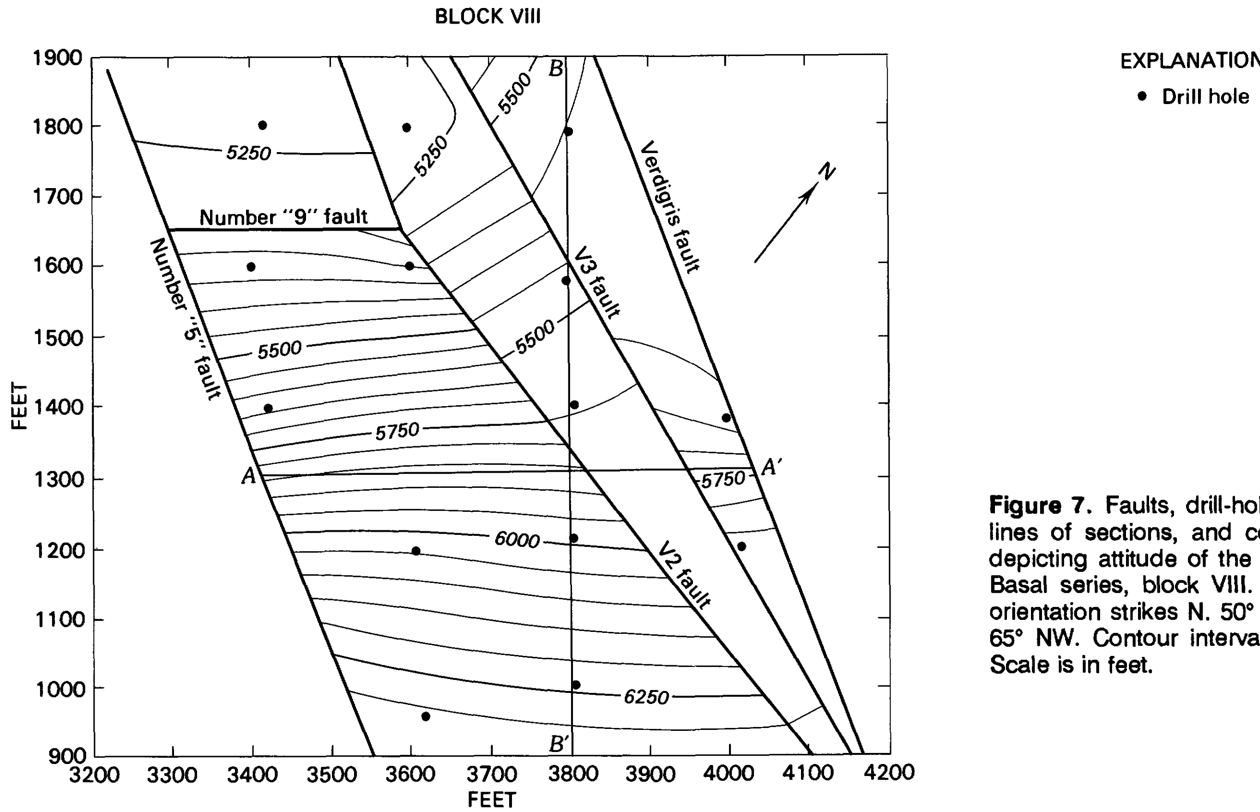

Figure 7. Faults, drill-hole locations, lines of sections, and contour lines depicting attitude of the base of the Basal series, block VIII. Block VIII's orientation strikes N. 50° E. and dips 65° NW. Contour interval is 50 feet. Scale is in feet.

A three-dimensional perspective of the base of the Basal series (fig. 7) is presented in figure 8. In order to observe the slope and have all features visible, the viewpoint of this perspective is 235° clockwise from north at an inclination of 20° from the horizontal. This faulted surface was computed using 14 vertical holes with a spatial distribution as shown in figure 7 and a deviation of the surface of less then 0.5 percent of the range of the true elevations. Elevations of areas outside of block VIII are to be ignored because these areas were not computed. The steep inclination of the base of the Basal series and the resultant effect of the minor faults are also shown in figure 8.

The spatial distribution and number of 25-foot intervals that vertical drill holes penetrate in the Basal series cumulate rocks is shown in a plan view (map) of block VIII in figure 9. In displaying thickness and areal extent of stratigraphic units, the convention used in figures 9 and 10 (and later in figs. 14 and 15) is that the lower case "b" or "c" denotes map areas above and below the Basal series-metasedimentary rock contact, respectively, and the number following "b"or "c"denotes thickness in terms of the number of 25-foot intervals for that area. In the earlier tables and the following discussion, upper case "B" and "C" represent 25-foot intervals above and below the Basal series-metasedimentary rock contact, respectively, with a numerical suffix indicating the specific interval away from the contact. Figure 9, oriented in the same manner as figure 7, shows that 3 of the 14 vertical drill holes (those in areas labeled b2) pass through two 25-foot intervals (B2 and B1), that one of the holes (in the area labeled b6) passes through six of the 25-foot intervals (B6, B5, B4, B3, B2, and B1), and so forth. The holes shown in figure 9, along with two inclined holes, were used in computing the grades presented in table 6 for block VIII.

Due to the inclination of the stratigraphy and exposure at the surface in block VIII, lithologies in the southeastern part of the block are truncated by erosion. Figure 9 represents the distribution of 25-foot intervals between the base of the Basal series and either the surface exposure or the base of the Ultramafic series. Erosion and inclination of the strata result in a thickness of the Basal series that goes from 50 feet (b2) to 200 feet (b8) above the base of the contact. As with the metasedimentary rocks below the Basal series, the 25-foot intervals are spatially limited by the stratigraphic information available in drill cores and at the surface. Since most holes are collared in the Ultramafic series and terminate in the underlying metasedimentary rock, an upward and downward limit to the thickness of the Basal series is defined. Surface erosion has eliminated the Ultramafic series and truncated the Basal series, affecting the four most easterly drill holes (shown as x's on fig. 9). For this reason, an originally much thicker Basal series in the eastern part of block VIII appears to pinch out in an easterly direction.

Figure 10 is a similar map of block VIII that shows the number of 25-foot intervals penetrated by drill holes in the metasedimentary rocks beneath the Basal series. It also shows two important features associated with the assigned thickness of cordierite-rich metasedimentary rocks below the base of the Basal series. First, it shows the spatial distribution of the thickness of the cordierite-rich metasedimentary rocks. Areas labeled c1, c2, and c3, which indicate the thickness of the cordierite-rich metasedimentary rocks, were used in computing tonnages. Drill holes in area c3 pass through three 25-foot intervals (C3, C2, and C1), holes in area c2 pass through two 25-foot intervals (C2 and C1), and holes in area c1 pass through the C1 interval. All holes start above the base of the Basal series, and most holes terminate in the underlying quartz-rich metasedimentary rocks. Therefore, the lower extent of the rocks of economic interest is known. The remaining holes either do not completely penetrate the cordierite-rich metasedimentary rocks or, as the two most southeasterly holes, go directly from the Basal series to quartz-rich metasedimentary rocks.

The second important feature of the metasedimentary rocks below the base of the Basal series concerns the relation between cordierite-rich and quartz-rich metasedimentary rocks. As can be seen in figure 10, cordierite-rich metasedimentary rocks appear to pinch out in an easterly and southerly direction. This pinching out may be a function of an original depositional relationship, folding of the metasedimentary rocks, or pre-intrusion erosion of a folded surface.

The pinching out of the Basal series due to surface erosion is apparent in figure 11, which shows the distribution of 25-foot intervals above and below the base of the Basal series along cross sections for block VIII. These cross sections correspond to the *A–A′*, *B–B′* traces as found in figures 7, 9, 10 and with the same perspective as figure 8. Figure 11 is included to give the reader a true composite view of the 25-foot intervals penetrated in block VIII, including surface orientations, fault locations, and distribution of the volumes of rock used in the grade-tonnage calculations.

Block IV is penetrated by eight vertical drill holes as shown in figure 12. One vertical drill hole used in the structural interpretation (fig. 3) was collared below the Basal series-metasedimentary rock contact; therefore, it was not used in the grade-tonnage calculations for block IV. The area of interest is delineated by the number "1" fault in the northwest, the unnamed fault in the northeast, the number "2" fault in the west, and exposure of the Basal series-metasedimentary rock contact due to erosion and inclination of the strata in the south. All faults are assumed to be vertical. Block IV has an area of approximately 292,300 square feet at the surface and 442,900 square feet at depth due to the 49° angle of inclination.

The orientation of block IV, based on the Ultramafic series-Basal series contact is N. 72° E., 49° NW. This orientation was calculated from the average of four three-point problems computed on six drill holes that penetrate the Ultramafic series-Basal series contact. A contour map of the base of the Basal series in block IV is shown in figure 12. The contact dips to the north from a surface exposure of approximately 6,450 feet above sea level to 6,160 feet before the number "1" fault is intercepted. A three-dimensional perspective view of this surface is shown in figure 13, from the same direction as figure 8, 235° clockwise rotation from north and 20° above the horizontal plane. This figure shows a perspective computed below a horizontal surface, however, in contrast to block VIII, which was computed above a horizontal surface or plane. These different views give additional insight into how the contact appears below the surface. Block IV has no apparent internal faults; however, a relatively smooth undulating base for the Basal series may be indicative of minor movement along faults. The Basal series of block IV becomes thinner further to the west, which could be indicative of an undulating cumulate floor or minor undetected faulting.

The distribution of the 25-foot intervals encountered in the Basal series in block IV is shown in figure 14. These thicknesses range from 75 feet (B3, B2, B1) in the east, where erosion has removed the overlying intervals, to 200 feet (B8 through B1 inclusive) to the west which reflects a thickening of the Basal series from east to west. The Basal series of block IV again becomes thinner further to the west.

The distribution of the cordierite-rich metasedimentary rocks and the number of 25-foot intervals penetrated is shown by figure 15. All holes shown in this section start above the Basal series-metasedimentary rock contact and terminate in the quartz-rich metasedimentary rocks below; therefore, complete sections of cordierite-rich metasedimentary rocks are identified. A thinning of cordierite-rich metasedimentary rocks is present. Where the cordierite-rich unit is absent in one drill hole, the Basal series rests directly on quartz-rich metasedimentary rocks. Cordierite-rich metasedimentary rocks appear to be thicker in both an easterly (areas denoted C2a, C3a, and C4a) and westerly (areas denoted C2, C3, and C4) direction from this point. Tonnages were computed separately for the rock units in the areas in the eastern part of block IV that are denoted with the lower case "a" suffix in figure 15. Because the southern exposure of the study area is the surface exposure of the base of the Basal series, erosion does not truncate these metasedimentary rocks north of the surface contact.

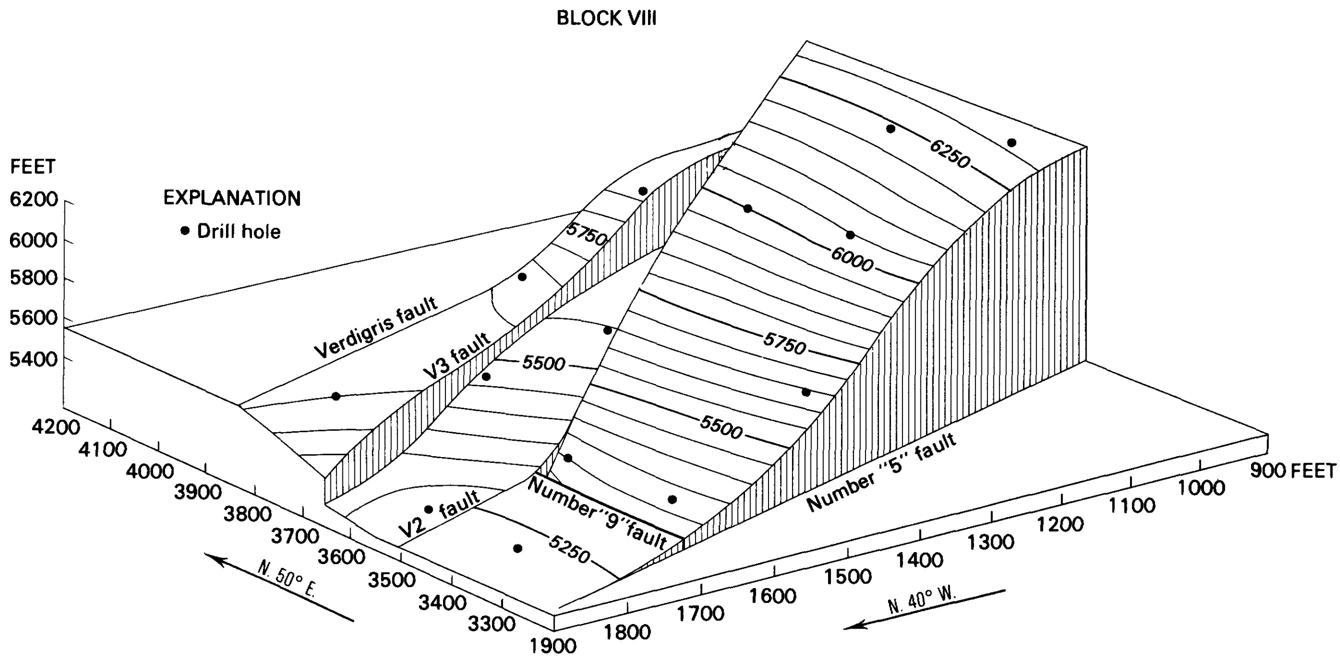

Figure 8. Three-dimensional perspective view of the base of the Basal series, block VIII; inclination is 20°, rotation 235°. Perspective is above a horizontal plane. Contour interval is 50 feet.

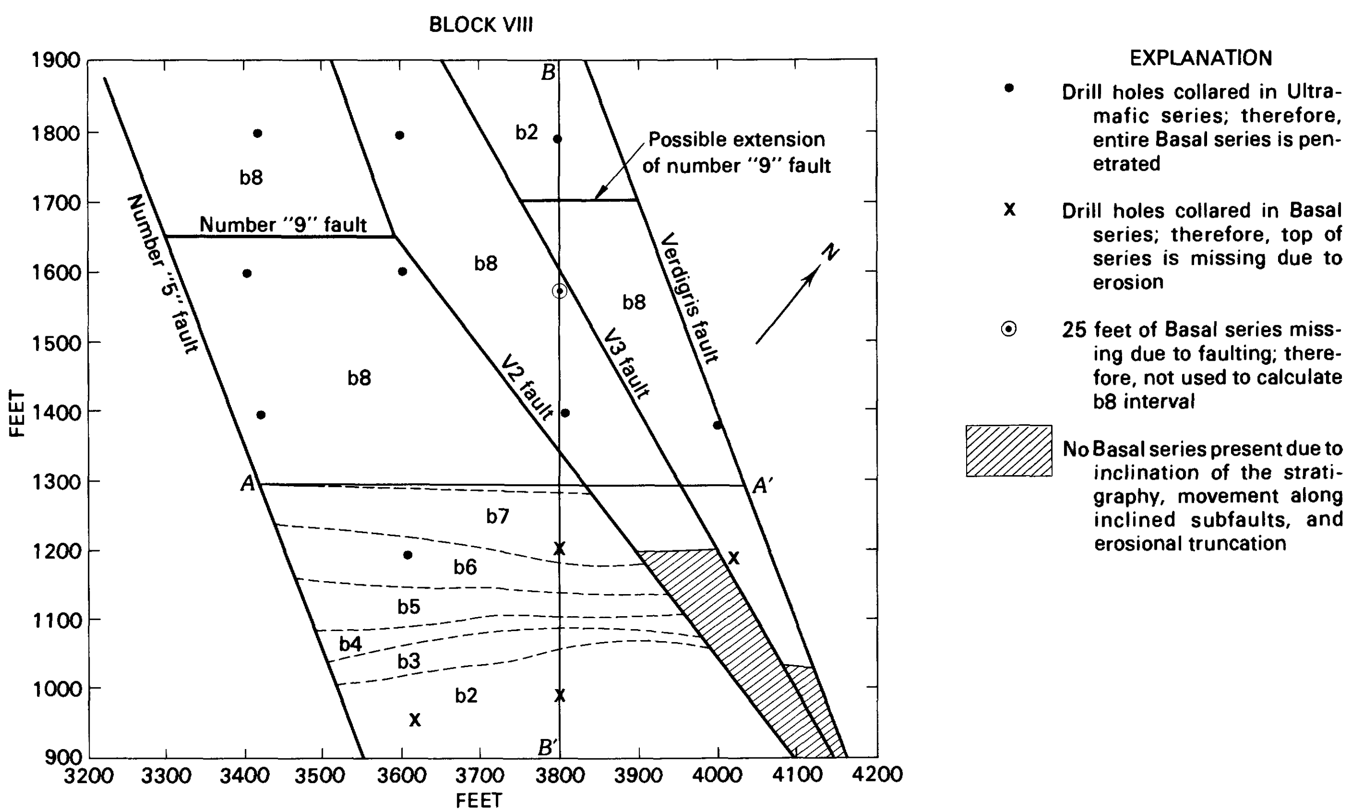

Figure 9. Spatial distribution of 25-foot intervals above the base of the Basal series used in grade-tonnage calculations for block VIII. B8 represents the uppermost 25-foot interval considered conformable to the Basal series-metasedimentary rock contact. Drill holes shown in b8 have penetrated intervals B1 through B8. Those shown in b7 have penetrated B1 through B7, and so on (b2 is inclusive of b1). All holes penetrate the base of the Basal series. Scale is in feet.

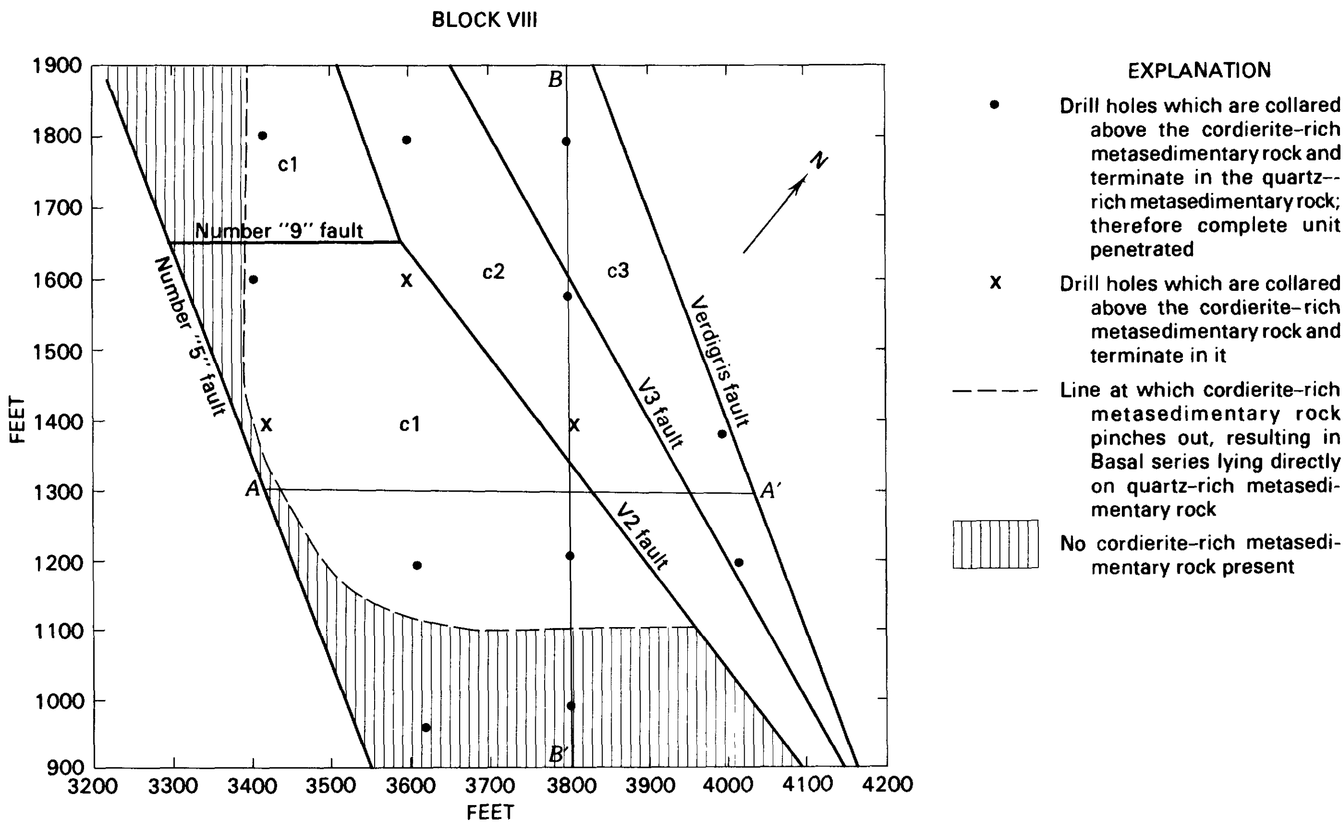

Figure 10. Spatial distribution of 25-foot intervals below the base of the Basal series in the cordierite-rich metasedimentary rocks used in grade-tonnage calculations for block VIII. C1 represents the uppermost 25-foot interval conformable to the Basal series-metasedimentary rock contact. Drill holes shown in c3 have penetrated intervals C1 through C3. Those shown in c2 have penetrated C1 and C2, and those shown in c1 have penetrated only C1. Scale is in feet.

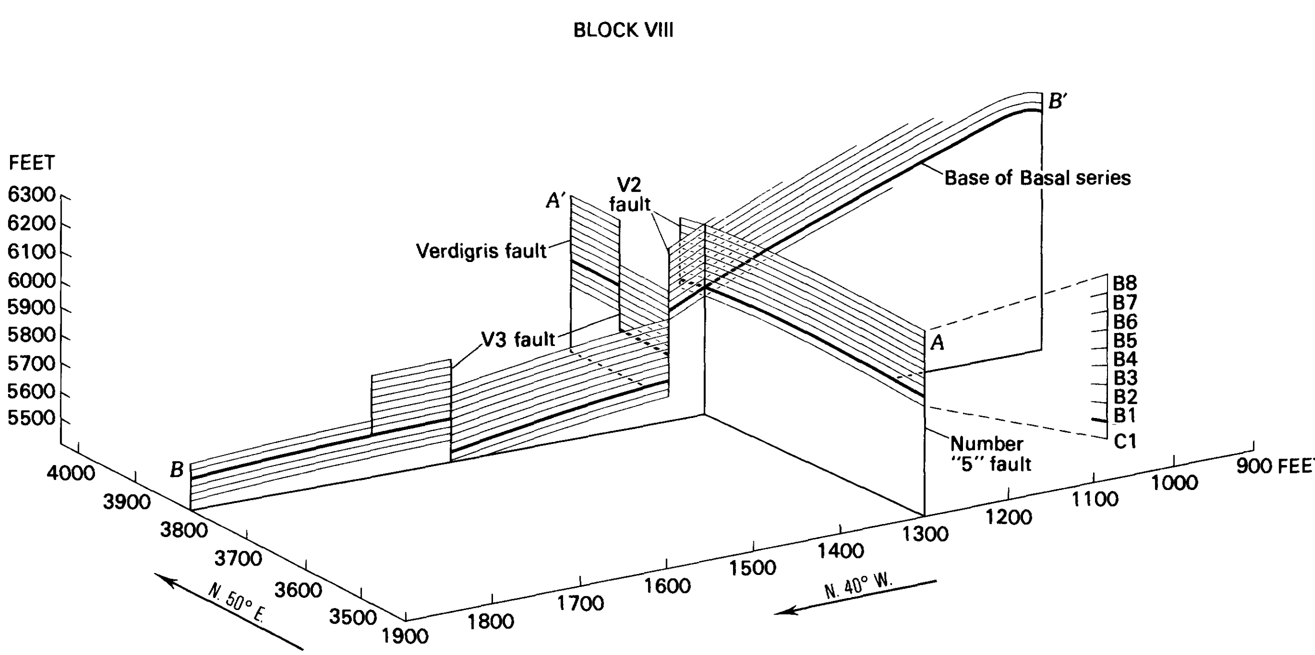

Figure 11. Cross sections *A–A′* and *B–B′* through block VIII showing the distribution of 25-foot intervals away from the base of the Basal series and used in grade-tonnage calculations.

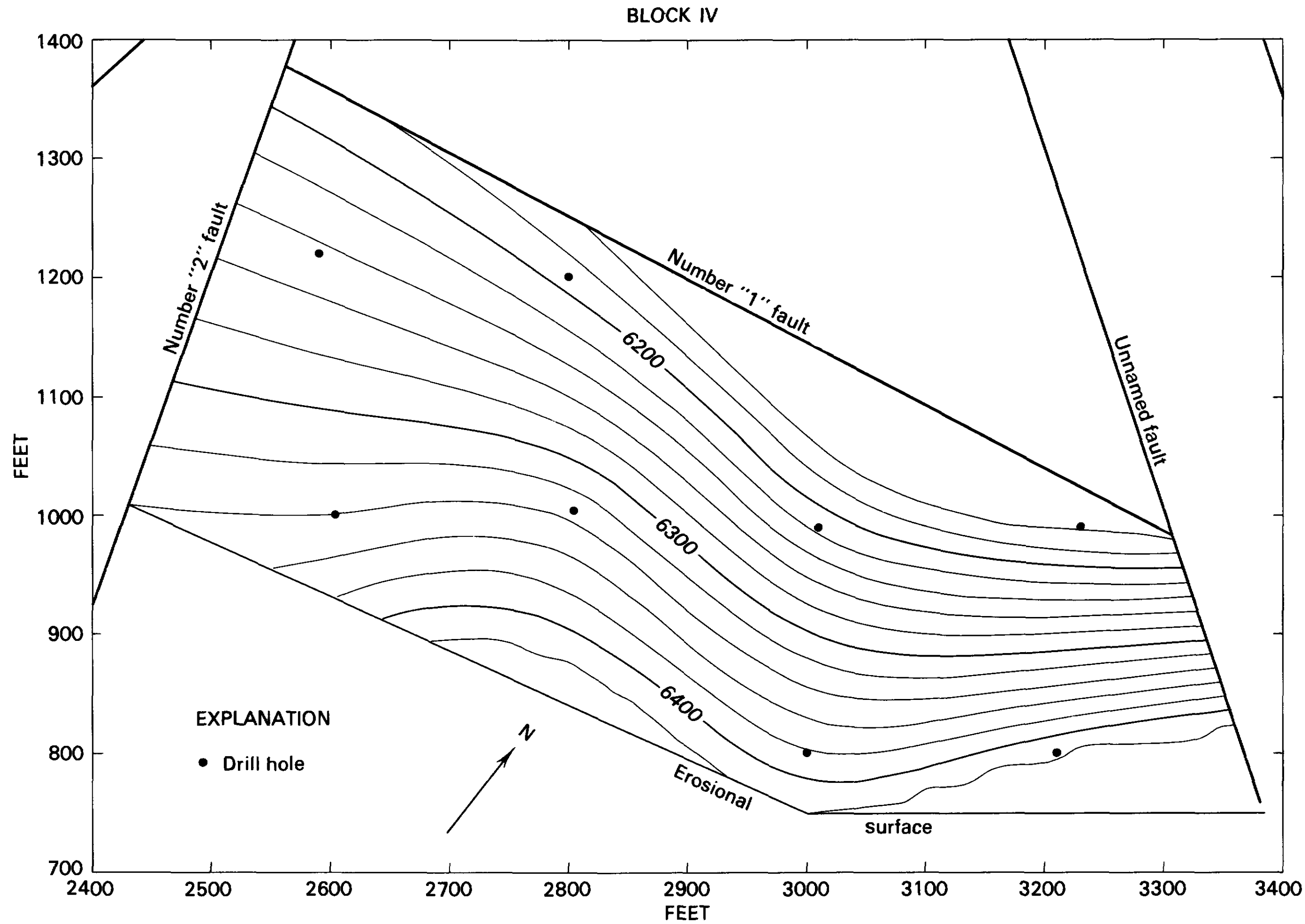

Figure 12. Faults, drill-hole locations, lines of sections, and contour lines depicting attitude of the base of the Basal series, block IV. Block IV strikes N. 72° E. and dips 49° NW. Contour interval is 20 feet. Scale is in feet.

Methods of Appraisal

Each fault-bounded block examined in detail was subdivided into 25-foot intervals which were spatially limited as described previously. These 25-foot intervals were then subdivided by 25-foot and 100-foot square grids. These subdivisions resulted in mining blocks 25×25×25 feet and 25×100×100 feet for the computations. Concentration data from scattered drill holes within each fault-bounded block were used to interpolate grades between drill holes for each mining block. Assuming a rock density of 0.0952 short tons per cubic foot (3.05 grams per cubic centimeter)(Kleinkopf, 1985), a tonnage was associated with each mining block. An inventory of mining blocks and their assigned copper and nickel grades was made. For specific combined copper and nickel cutoff grades (for each 25-foot layer), the total ore tonnage was computed along with the associated average copper and nickel grades (tables 7, 8).

Sample grades for each drill hole intersecting each 25-foot interval were calculated by using a weighted mean for the copper and nickel values present. Methods used for extending sample grades to estimate the mining block grades were quite primitive because of the scarcity of data. As table 6 indicates, the numbers of observations in any individual fault-bounded block and 25-foot interval were very limited. Attempts to estimate a well behaved variogram for the 100-foot horizontal layers across the study area shown in tables 2 and 3 were unsuccessful. Consequently, geostatistical methods could not be applied to quantify probabilistically the confidence attached to grade or tonnage estimates. Methods used for extending the sample data to individual mining blocks were (1) the inverse distance algorithm, (2) the inverse distance squared algorithm, and (3) the algorithm used in the commercially available Interactive Surface Modeling Program (Dynamic Graphics, 1984). Each method or procedure weights data in order to compute estimates of the copper or nickel grade for points located at the center of each mining block. These values are then assumed to be the average grade value for the particular block. In

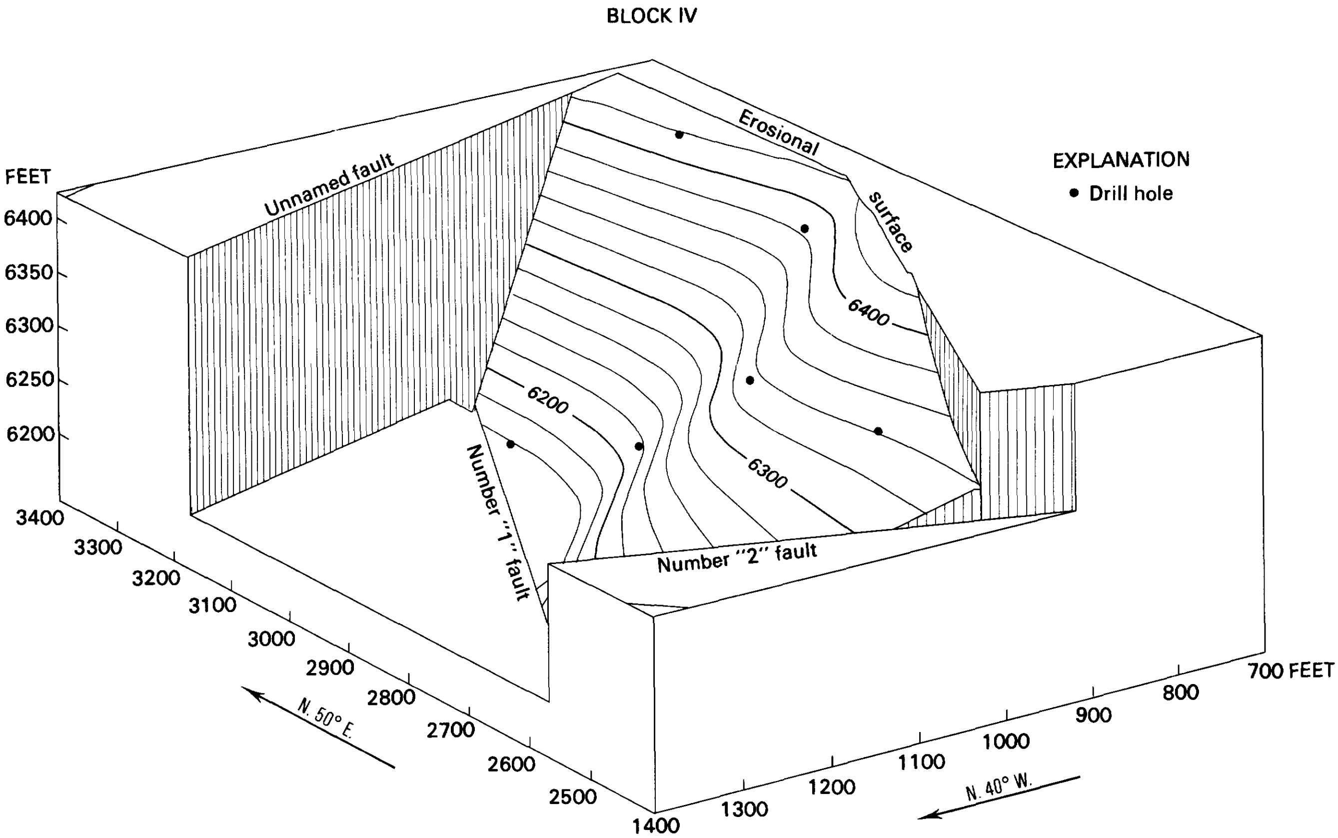

Figure 13. Three-dimensional perspective view of the base of the Basal series, block IV; inclination is 20°, rotation 235°. Perspective is below a horizontal plane. Contour interval is 20 feet.

applying these methods, we have assumed continuous mineralization between drill holes.

Application of the inverse distance method assumes that there are relationships between the grade of a hole and the grade of adjoining blocks and that the relationship can be expressed as some function of distance between the two. Grades from all surrounding holes are used in estimating the block grade. Weights of each surrounding hole value are determined by distance between the drill hole and the block under consideration. Particular weights are inversely proportional to this distance;

that is, $Z_k^* = \dfrac{\sum \frac{Z_i}{d_{ik}}}{\sum \frac{1}{d_{ik}}}$

where

Z_k^* is the block grade,

Z_i is the i-th hole grade, and

d_{ik} is the distance between the i-th hole and center of the k-th block.

Even more weight can be attached to the samples nearer the block by squaring the distance between the k-th block and the i-th sample. Thus, the formula for the inverse distance squared weighting scheme is

$$Z_k^* = \frac{\sum \frac{Z_i}{d_{ik}^2}}{\sum \frac{1}{d_{ik}^2}}$$

where Z_k^*, Z_i and d_{ik} are defined as above.

Finally, with some restrictions of extreme values, the Interactive Surface Modeling Program algorithm iteratively fits progressively more complicated mathematical functions to the data until there is no longer any additional improvement in the fit to the sample data. For a technical description of the algorithm, see Briggs (1974). This algorithm will extrapolate (linear or nonlinear) trends beyond the edges of the sample space, whereas the inverse distance and inverse distance squared methods extrapolate constant values beyond the area bounded by data points.

Grade-Tonnage Relations for Block VIII

Table 6 shows the number of holes in each of the 25-foot intervals in fault block VIII. Tonnages were computed for intervals B1 through B8 (200 feet above the base of the Basal series) and C1 through C3 (75 feet below the base of the Basal series). In figures 16 and 17,

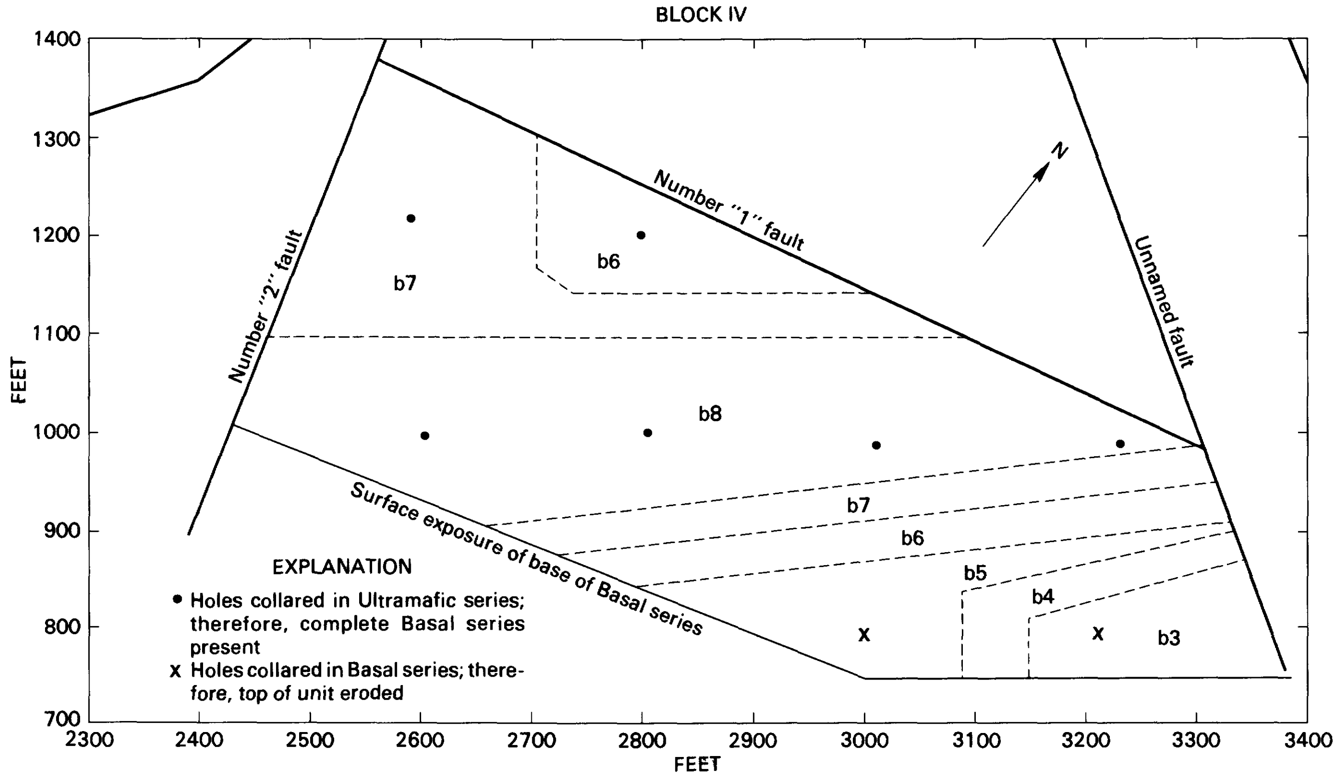

Figure 14. Spatial distribution of 25-foot intervals above the base of the Basal series used in grade-tonnage calculations for block IV. B8 represents the uppermost 25-foot interval conformable to the Basal series-metasedimentary rock contact. Drill holes shown in b8 have penetrated intervals B1 through B8. Those shown in b7 have penetrated intervals B1 through B7, and so on (b3 is inclusive of b1 and b2). All holes penetrate the bottom of the Basal series. Block IV strikes N. 72° E. and dips 49° NW. Scale is in feet.

computations were based on mining blocks assumed to be 100×100 feet and to have a thickness of 25 feet. Results in figures 18 and 19 are based on the assumption that the mining blocks are cubes 25 feet on each side. The results of the inverse distance, inverse distance squared, and Interactive Surface Modeling algorithms on the cutoff grade-tonnage computations for combined copper and nickel are shown in figures 16 and 18. Figures 17 and 19 show the average grade (combined copper and nickel) at each tonnage corresponding to the cutoff grade tonnages from the inverse distance, inverse distance squared, and Interactive Surface Modeling algorithms shown in figures 16 and 18. Figure 16 indicates that above and below approximately a 0.4-percent cutoff grade, the estimated tonnages computed by the three methods diverge. At a combined copper and nickel cutoff grade of 0.5 percent, the estimated ore tonnages are within 10 percent of each other, whereas at a 0.2-percent cutoff grade, the Interactive Surface Modeling algorithm shows tonnages at least 10 percent below the results computed by the other two algorithms. The cutoff grade-tonnage relations computed by all three methods were not very sensitive to mining block size as seen from a comparison of figures 16 and 18.

To estimate the grade-tonnage relations displayed in figures 16 and 18, the procedure was to first specify a combined cutoff grade and then calculate the tonnage in all those mining blocks having average grades at least as high as the cutoff grade. Figures 17 and 19 present the average combined copper and nickel grades for the tonnages shown in figures 16 and 18.

Figure 20 shows average copper and nickel grades as a function of the tonnages computed on the basis of the inverse distance squared method using 25-foot cubic mining blocks. Average nickel grades in figure 20 are always higher than average copper grades. Average nickel grades were also higher than the average copper grades when the inverse distance and the Interactive Surface Modeling algorithms were used. Metal content of ore tonnages associated with each cutoff grade can be calculated using data presented in these figures. Using these figures for the inverse distance squared method, at the combined average grade of 0.50 percent copper and nickel (fig. 19), estimated ore tonnage was 19.7 million short tons. According to the data used to generate figure 20, the corresponding average copper grade is then 0.235 percent, and the nickel grade is 0.265 percent. Consequently, the estimated in situ copper metal tonnage is 46,300 short tons, and nickel metal tonnage is 52,200 short tons.

Table 7 shows the results for block VIII of the three algorithms applied to each 25-foot interval and areas

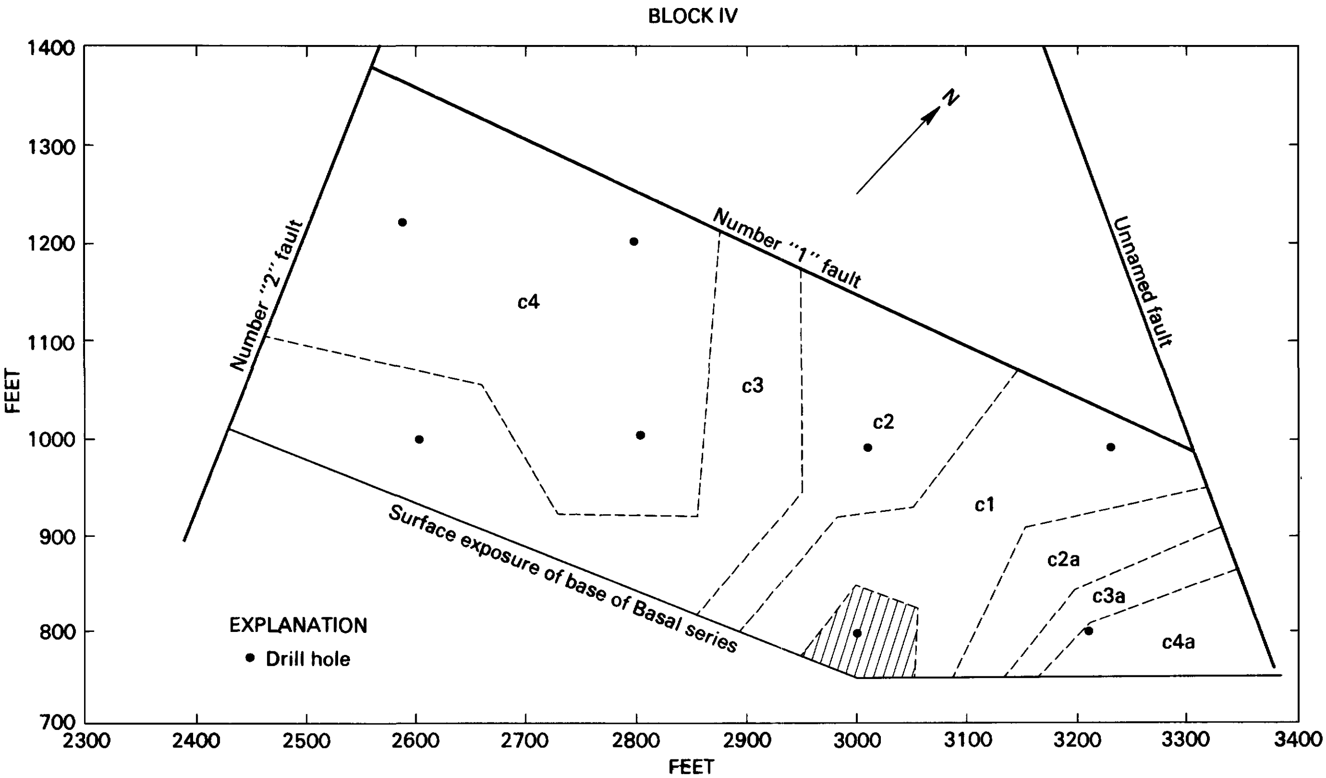

Figure 15. Spatial distribution of 25-foot intervals below the base of the Basal series used in grade-tonnage calculations for block IV. Shaded area represents Basal series which rests directly on quartz-rich hornfels; therefore, no cordierite-rich hornfels are present. Block IV strikes N. 72° E. and dips 49° NW. All drill holes penetrate quartz-rich hornfels. C1 represents the uppermost 25-foot interval conformable to the Basal series-metasedimentary rock contact. Drill holes shown in c3 have penetrated intervals C1 through C3. Those shown in c2 have penetrated through C1 and C2, and those shown in c1 have penetrated only C1. For interpretation for areas c2a, c3a, and c4a, see the text. Scale is in feet.

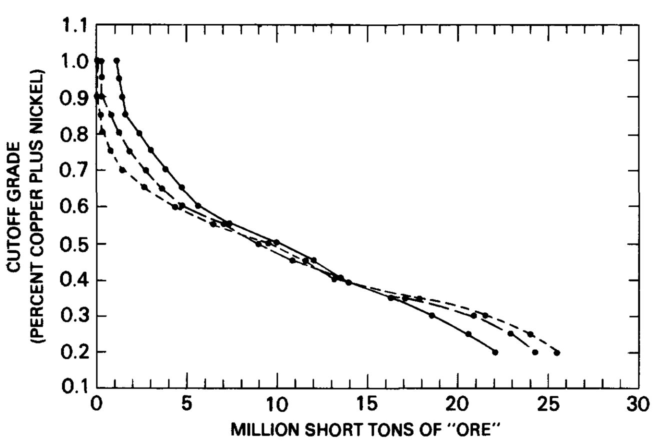

Figure 16. Cutoff grade (combined copper and nickel) vs. ore tonnage, computed using the Interactive Surface Modeling algorithm (solid line), the inverse distance squared algorithm (long dashes), and the inverse distance algorithm (short dashes), for block VIII. Mining blocks are 100×100×25 feet.

delineated and displayed in figures 9 and 10. For each combined cutoff grade (0.8 percent, 0.6 percent, 0.4 percent, and 0.2 percent), the corresponding ore tonnage and the average copper and nickel grades are computed. In general, as one moves further away from the Basal series-metasedimentary rock contact, ore tonnage tends to decline. This occurs for two reasons. First, as shown by table 6, the concentration grades tend to decline as the distance from the contact increases, so that a progressively larger fraction of tonnage will be classified as waste rock. Second, because of irregular stratigraphy, faulting, and erosion within block VIII, the plan view surface areas corresponding to each 25-foot layer decline as distances from the contact increase.

The tonnage of all rock for each 25-foot interval can be computed by multiplying the product of the area of the interval and the thickness of interval (25 feet) by the weight per cubic foot (0.0952 short tons/cubic foot). For block VIII, this tonnage is 25.860 million tons of rock.

Table 7. Grades and tonnages for in situ ore in fault block VIII, computed by three algorithms

[Calculations are based on cubic blocks of 25 feet; - - -, no data. Rows labeled "Composite" represent average grade of the aggregate ore in all intervals and total ore tonnage at the specified cutoff grade]

25-foot interval	Area ($ft^2 \times 10^3$)	0.8% cutoff combined grade			0.6% cutoff combined grade			0.4% cutoff combined grade			0.2% cutoff combined grade		
		Avg. grade		Short tons ore ($\times 10^6$)	Avg. grade		Short tons ore ($\times 10^6$)	Avg. grade		Short tons ore ($\times 10^6$)	Avg. grade		Short tons ore ($\times 10^6$)
		Cu (%)	Ni (%)		Cu (%)	Ni (%)		Cu (%)	Ni (%)		Cu (%)	Ni (%)	
Inverse distance algorithm													
B8 ------	869.2	---	---	---	0.21	0.41	0.003	0.19	0.25	0.335	0.17	0.16	2.015
B7 ------	971.0	0.38	0.55	0.003	.29	.40	.046	.22	.27	.392	.18	.20	2.303
B6 ------	1,022.9	---	---	---	.38	.24	.003	.21	.22	.117	.16	.19	2.426
B5 ------	1,092.2	---	---	---	---	---	---	.17	.27	.028	.12	.16	2.576
B4 ------	1,127.9	---	---	---	.36	.35	.003	.22	.22	.364	.18	.18	2.675
B3 ------	1,165.5	---	---	---	.24	.42	.007	.20	.27	2.651	.20	.26	2.768
B2 ------	1,394.4	.40	.53	.054	.33	.36	.441	.27	.27	3.203	.27	.27	3.312
B1 ------	1,394.4	.43	.49	.163	.33	.36	2.784	.33	.34	3.301	.33	.34	3.312
*----------													
C1 ------	1,092.6	.25	.66	.023	.22	.47	.192	.23	.28	2.452	.22	.27	2.595
C2 ------	496.9	.65	.19	.003	.52	.16	.017	.34	.13	.242	.23	.10	1.075
C3 ------	238.7	---	---	---	---	---	---	.19	.22	.046	.16	.16	.551
Composite	---	.41	.51	.248	.32	.37	3.496	.26	.28	13.131	.21	.23	25.608
Inverse distance squared algorithm													
B8 ------	869.2	---	---	---	0.21	0.42	0.067	0.20	0.27	0.638	0.19	0.18	1.647
B7 ------	971.0	0.37	0.53	0.078	.33	.47	.155	.25	.32	.440	.18	.20	2.270
B6 ------	1,022.9	---	---	---	.38	.24	.003	.22	.23	.495	.16	.20	2.384
B5 ------	1,092.2	---	---	---	---	---	---	.18	.28	.223	.13	.17	2.329
B4 ------	1,127.9	---	---	---	.33	.32	.043	.23	.24	.752	.18	.19	2.622
B3 ------	1,165.5	---	---	---	.24	.40	.138	.21	.29	2.278	.20	.27	2.768
B2 ------	1,394.4	.47	.59	.234	.38	.41	.778	.29	.29	2.751	.27	.28	3.200
B1 ------	1,394.4	.46	.53	.495	.36	.40	2.185	.34	.36	3.075	.33	.34	3.274
*----------													
C1 ------	1,092.6	.25	.72	.149	.23	.54	.460	.24	.32	1.936	.23	.28	2.574
C2 ------	496.9	.65	.19	.028	.55	.17	.131	.42	.15	.367	.29	.12	.799
C3 ------	238.7	---	---	---	---	---	---	.20	.23	.192	.18	.19	.476
Composite	---	.43	.56	.984	.35	.41	3.960	.27	.30	13.147	.22	.24	24.343
Interactive surface modeling algorithm													
B8 ------	869.2	---	---	---	0.21	0.44	0.081	0.21	0.28	1.019	0.20	0.23	1.539
B7 ------	971.0	0.40	0.58	0.144	.36	.51	.238	.26	.33	.734	.19	.22	1.960
B6 ------	1,022.9	---	---	---	.37	.24	.007	.23	.24	.921	.18	.21	2.270
B5 ------	1,092.2	---	---	---	.19	.41	.014	.19	.31	.572	.15	.20	1.841
B4 ------	1,127.9	---	---	---	.33	.32	.254	.26	.27	1.042	.20	.20	2.225
B3 ------	1,165.5	---	---	---	.24	.44	.691	.23	.34	2.035	.21	.29	2.768
B2 ------	1,394.4	.51	.56	.597	.45	.45	1.065	.36	.35	2.054	.29	.29	3.065
B1 ------	1,394.4	.45	.55	1.072	.40	.47	1.906	.36	.41	2.571	.33	.36	3.108
*----------													
C1 ------	1,092.6	.36	.83	.573	.33	.64	.996	.32	.45	1.738	.28	.37	2.346
C2 ------	496.9	.67	.21	.152	.60	.19	.283	.51	.17	.458	.42	.14	.673
C3 ------	238.7	---	---	---	---	---	---	.21	.23	.182	.17	.10	.487
Composite	---	.45	.60	2.538	.38	.47	5.535	.30	.34	13.326	.24	.27	22.282

*Dashed lines denote contact between Basal series and cordierite-rich metasedimentary rocks.

Table 8. Grades and tonnages for in situ ore in fault block IV, computed by three algorithms

[Calculations are based on cubic blocks of 25 feet; ---, no data. Rows labeled "Composite" represent average grade of the aggregate ore in all intervals and total ore tonnage at the specified cutoff grade]

25-foot interval	Area ($ft^2 \times 10^3$)	0.8% cutoff combined grade			0.6% cutoff combined grade			0.4% cutoff combined grade			0.2% cutoff combined grade		
		Avg. grade		Short tons ore ($\times 10^6$)	Avg. grade		Short tons ore ($\times 10^6$)	Avg. grade		Short tons ore ($\times 10^6$)	Avg. grade		Short tons ore ($\times 10^6$)
		Cu (%)	Ni (%)		Cu (%)	Ni (%)		Cu (%)	Ni (%)		Cu (%)	Ni (%)	
Inverse distance algorithm													
B6 ------	369.3	---	---	---	---	---	---	---	---	---	0.11	0.13	0.412
B5 ------	416.8	---	---	---	---	---	---	0.17	0.26	0.011	.13	.17	.982
B4 ------	435.5	---	---	---	---	---	---	.18	.24	.007	.14	.17	1.032
B3 ------	465.1	0.34	0.49	0.002	0.28	0.40	0.027	.20	.27	.272	.16	.20	1.103
B2 ------	465.1	---	---	---	.39	.25	.002	.24	.21	.096	.17	.18	1.105
B1 ------	465.1	---	---	---	---	---	---	.22	.23	1.035	.21	.23	1.105
*													
C1 ------	450.7	---	---	---	.26	.39	.019	.22	.26	.881	.21	.24	1.068
C2 ------	323.8	---	---	---	.25	.38	.002	.19	.24	.223	.17	.21	.764
C3 ------	266.3	---	---	---	.35	.26	.002	.26	.20	.032	.17	.13	.608
C4 ------	154.3	---	---	---	---	---	---	---	---	---	.13	.15	.346
C2A-----	59.4	.52	.34	.013	.40	.30	.110	.38	.29	.141	.38	.29	.141
C3A-----	35.5	---	---	---	.41	.24	.034	.37	.22	.084	.37	.22	.084
C4A-----	21.5	.53	.54	.051	.53	.54	.051	.53	.54	.051	.53	.54	.051
Composite	---	.52	.50	.066	.40	.36	.245	.23	.25	2.833	.17	.19	8.801
Inverse distance squared algorithm													
B6 ------	369.3	---	---	---	---	---	---	---	---	---	0.12	0.15	0.427
B5 ------	416.8	---	---	---	---	---	---	0.17	0.27	0.081	.13	.18	.906
B4 ------	435.5	---	---	---	---	---	---	.18	.25	.074	.15	.18	.953
B3 ------	465.1	0.38	0.56	0.034	0.32	0.47	0.092	.23	.32	.337	.16	.21	1.053
B2 ------	465.1	---	---	---	.37	.24	.021	.26	.22	.221	.17	.18	1.089
B1 ------	465.1	---	---	---	.32	.28	.007	.23	.23	.817	.22	.22	1.089
*													
C1 ------	450.7	---	---	---	.28	.42	.099	.24	.28	.738	.22	.25	.981
C2 ------	323.8	---	---	---	.25	.39	.021	.20	.26	.270	.17	.22	.670
C3 ------	266.3	---	---	---	.35	.26	.002	.28	.21	.066	.16	.13	.460
C4 ------	154.3	---	---	---	---	---	---	---	---	---	.12	.14	.265
C2A-----	59.4	.55	.36	.119	.55	.35	.129	.55	.35	.129	.55	.35	.129
C3A-----	35.5	---	---	---	.47	.27	.074	.47	.27	.074	.47	.27	.074
C4A-----	21.5	.71	.72	.044	.71	.72	.044	.71	.72	.044	.71	.72	.044
Composite	---	.56	.47	.197	.43	.40	.489	.26	.27	2.871	.18	.20	8.140
Interactive surface modeling algorithm													
B6 ------	369.3	---	---	---	---	---	---	---	---	---	0.13	0.16	0.418
B5 ------	416.8	---	---	---	---	---	---	0.17	0.27	0.210	.14	.19	.805
B4 ------	435.5	---	---	---	---	---	---	.19	.25	.297	.16	.19	.789
B3 ------	465.1	0.38	0.55	0.117	0.33	0.48	0.216	.28	.39	.389	.19	.25	.942
B2 ------	465.1	---	---	---	.38	.25	.025	.25	.23	.293	.17	.18	1.105
B1 ------	465.1	---	---	---	.33	.30	.074	.26	.24	.723	.22	.22	1.105
*													
C1 ------	450.7	.35	.49	.061	.32	.40	.187	.28	.29	.834	.26	.26	.998
C2 ------	323.8	---	---	---	.24	.39	.027	.20	.28	.367	.18	.25	.572
C3 ------	266.3	---	---	---	.37	.29	.029	.28	.25	.123	.20	.18	.322
C4 ------	154.3	.75	.76	.001	.75	.76	.001	.20	.26	.035	.14	.18	.174
C2A-----	59.4	.60	.37	.094	.56	.35	.123	.53	.33	.141	.53	.33	.141
C3A-----	35.5	---	---	---	.49	.28	.074	.49	.28	.074	.46	.26	.084
C4A-----	21.5	.77	.78	.044	.77	.78	.044	.70	.70	.051	.70	.70	.051
Composite	---	.49	.52	.317	.40	.41	.800	.27	.29	3.537	.20	.22	7.506

*Dashed lines denote contact between Basal series and cordierite-rich metasedimentary rocks.

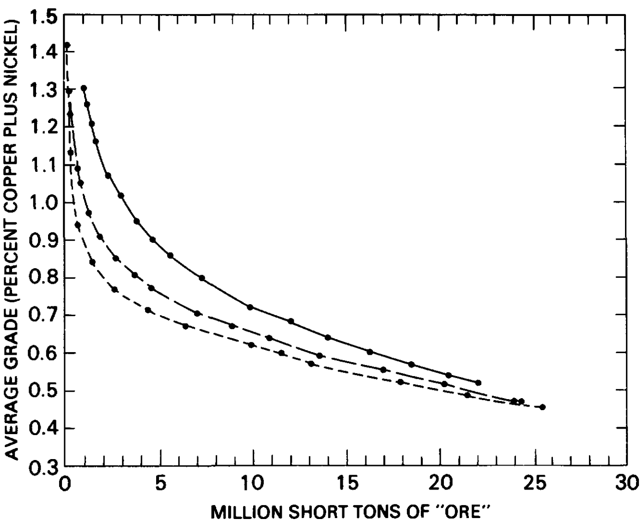

Figure 17. Average grade (combined copper and nickel) vs. ore tonnage, computed using the Interactive Surface Modeling algorithm (solid line), the inverse distance squared (long dashes), and the inverse distance algorithm (short dashes), for block VIII. Mining blocks are 100×100×25 feet.

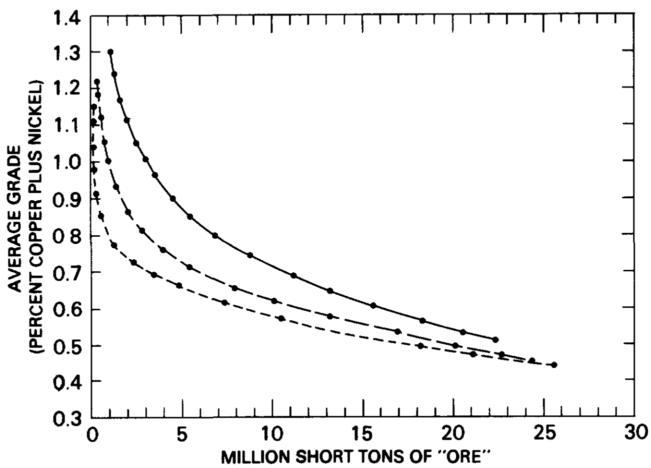

Figure 19. Average grade (combined copper and nickel) vs. ore tonnage, computed using the Interactive Surface Modeling algorithm (solid line), the inverse distance squared algorithm (long dashes), and the inverse distance algorithm (short dashes), for block VIII. Mining blocks are 25×25×25 feet.

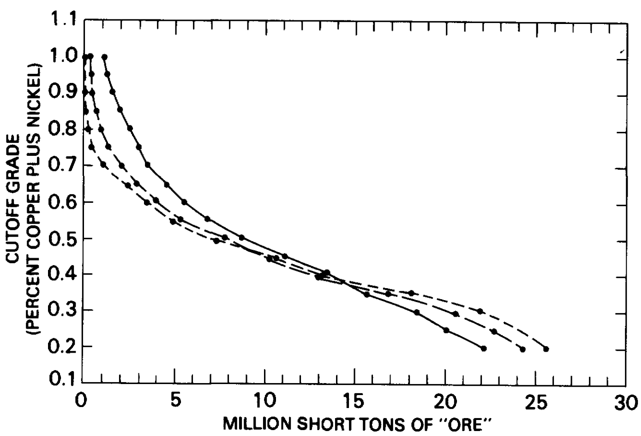

Figure 18. Cutoff grade (combined copper and nickel) vs. ore tonnage, computed using the Interactive Surface Modeling algorithm (solid line), the inverse distance squared algorithm (long dashes), and the inverse distance algorithm (short dashes), for block VIII. Mining blocks are 25×25×25 feet.

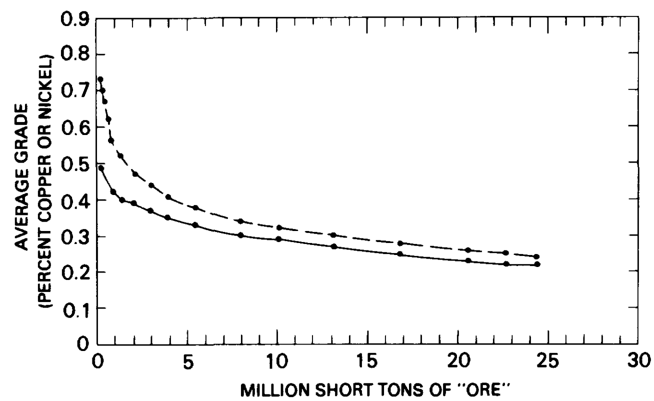

Figure 20. Average copper and average nickel grades vs. ore tonnage computed with the inverse distance squared algorithm for block VIII. Mining blocks are 25×25×25 feet. Solid line represents copper. Dashed line represents nickel.

Results computed with the inverse distance, inverse distance squared, and Interactive Surface Modeling algorithms (table 7) show that at the 0.4-percent combined copper and nickel cutoff grade, the waste rock (mining blocks having average grades below cutoff grades) accounts for almost half of the total tonnage delineated within the stratigraphic rock layers. At a 0.2-percent combined copper and nickel cutoff grade, only about 6 percent of the rock is waste using the inverse distance squared algorithm. At both cutoff grades of 0.4-percent and 0.2-percent combined copper and nickel, the fraction of rock that is waste typically increases with the distance away from the Basal series-metasedimentary rock contact.

The ore and metal tonnage that can be computed from table 7 represents in situ tonnages and does not account for losses due to engineering or to economic requirements associated with the mining or metallurgical recovery of the metal from the ore. Moreover, because there are only eight, seven, and four observations for intervals B8, C2, and C3 (table 6), respectively, tonnage

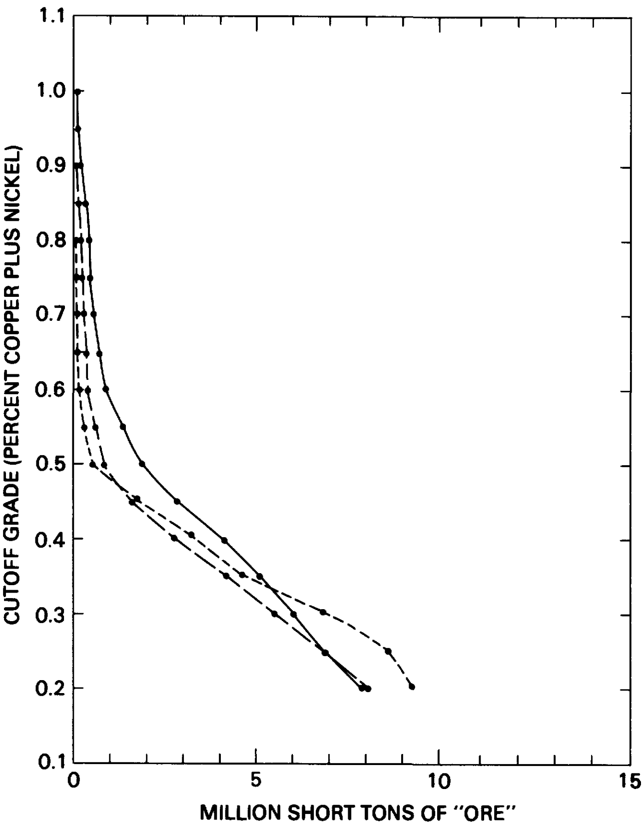

Figure 21. Cutoff grade (combined copper and nickel) vs. ore tonnage, computed using the Interactive Surface Modeling algorithm (solid line), the inverse distance squared algorithm (long dashes), and the inverse distance algorithm (short dashes), for block IV. Mining blocks are 100×100×25 feet.

estimates for these layers are based on relatively sparse data. Because we assumed that all faults are vertical, the surface area of each 25-foot interval is invariant with respect to depth. This assumption introduces a bias because the V2 and V3 faults trend northward toward the Verdigris fault with each successive interval away (upward) from the base of the Basal series. This trend of the V2 and V3 faults is also true below the base of the Basal series in the cordierite-rich metasedimentary rocks where these faults trend southward. Because no significant volume differences would be expected with the 25-foot intervals due to trending of these faults, however, this phenomenon was considered insignificant.

Grade-Tonnage Relations for Block IV

The surface area of the Basal series-metasedimentary rock contact in block IV (see figs. 12–15) is slightly less than one-third the surface area of rock layers in block VIII. As is the case for block VIII, the number of drill holes penetrating the base of the Basal series contact

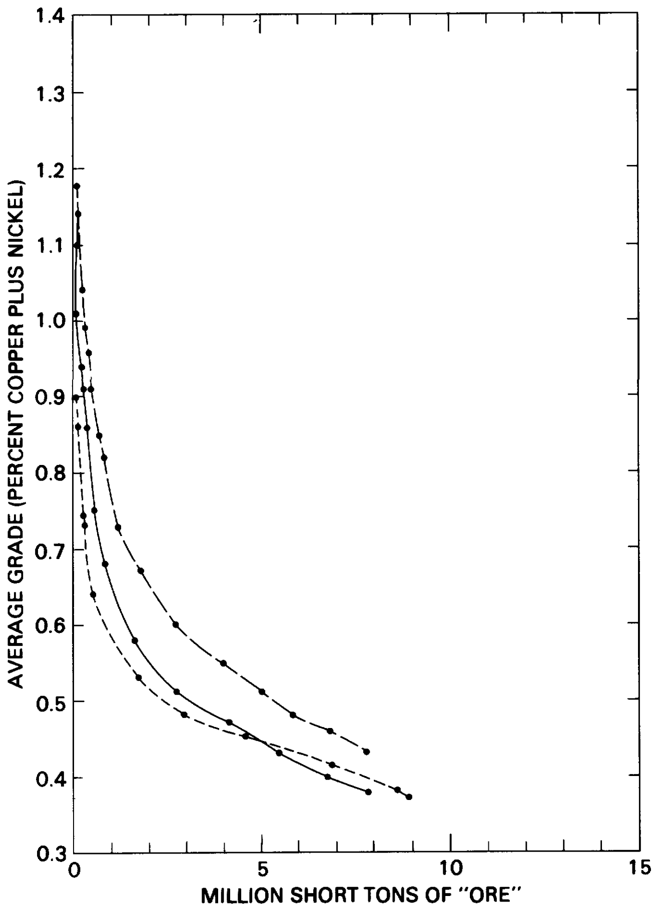

Figure 22. Average grade (combined copper and nickel) vs. ore tonnage, computed using the Interactive Surface Modeling algorithm (solid line), the inverse distance squared algorithm (long dashes), and the inverse distance algorithm (short dashes), for block IV. Mining blocks are 100×100×25 feet. For clarity in presentation, data points and curves representing tonnages smaller than 100,000 short tons are not shown.

in block IV is relatively sparse. The 25-foot layers examined for block IV were B1 through B6 and C1 through C3. Results of the grade-tonnage calculations using the three algorithms described earlier for block VIII are presented for block IV in figures 21–25 and in table 8. Figures 21 and 23 show the relations between the combined cutoff grades and their associated ore tonnages, and figures 22 and 24 show the relations between ore tonnage and average copper and nickel grades. These figures were drawn to the same scale as figures 16–19 to allow comparison of the grade-tonnage relations between blocks IV and VIII.

The results obtained with the inverse distance, inverse distance squared, and Interactive Surface Modeling algorithms were quite similar to each other. Also, the results show relatively little (10 percent) variation with respect to the assumed mining block size when comparing

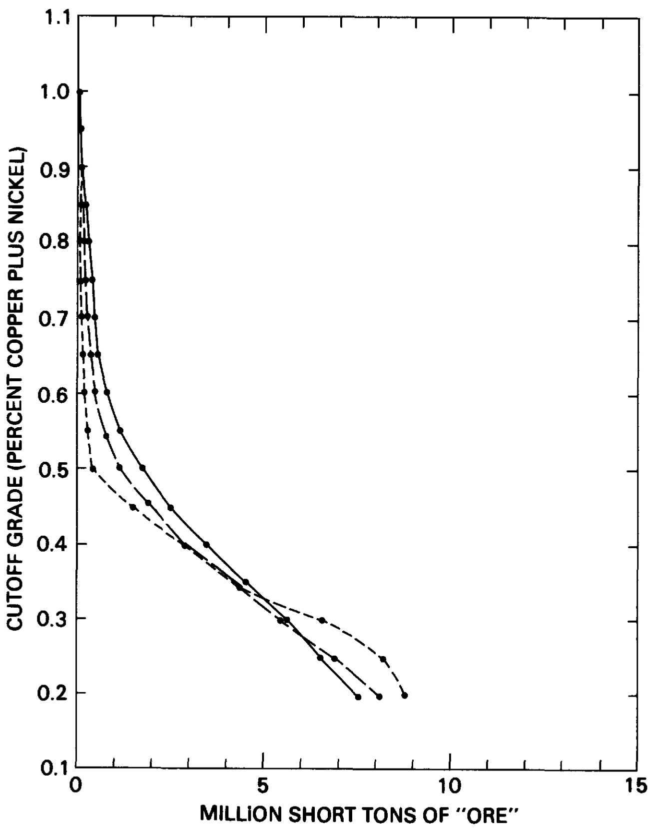

Figure 23. Cutoff grade (combined copper and nickel) vs. ore tonnage, computed using the Interactive Surface Modeling algorithm (solid line), the inverse distance squared algorithm (long dashes), and the inverse distance algorithm (short dashes), for block IV. Mining blocks are 25×25×25 feet.

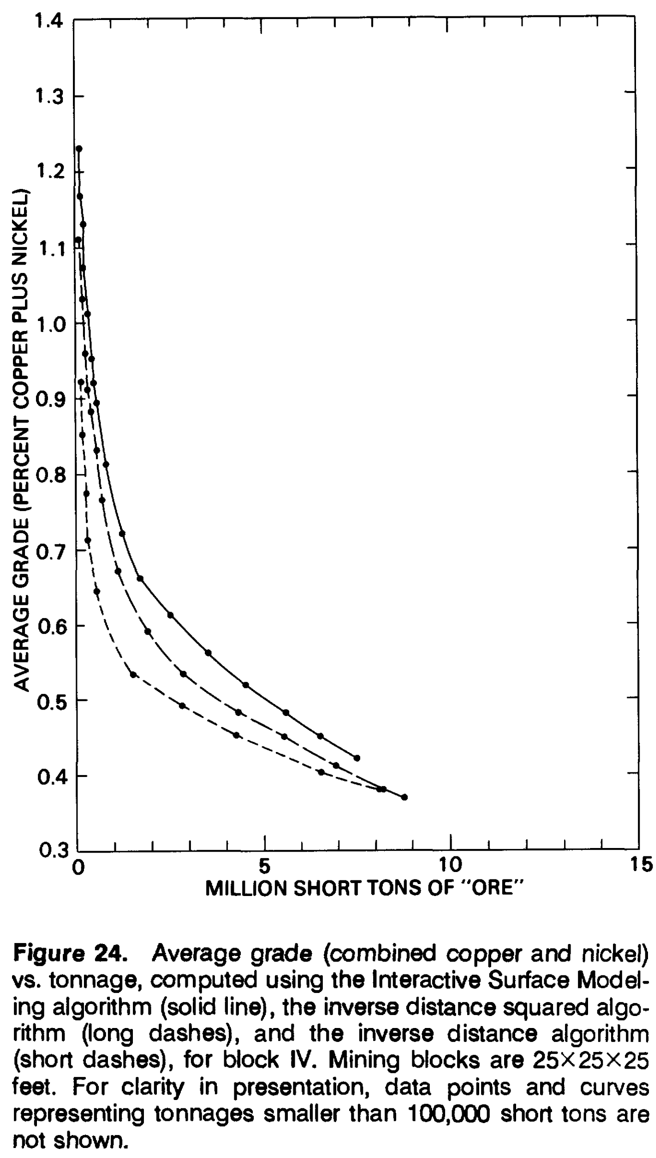

Figure 24. Average grade (combined copper and nickel) vs. tonnage, computed using the Interactive Surface Modeling algorithm (solid line), the inverse distance squared algorithm (long dashes), and the inverse distance algorithm (short dashes), for block IV. Mining blocks are 25×25×25 feet. For clarity in presentation, data points and curves representing tonnages smaller than 100,000 short tons are not shown.

figures 22 and 24. For example, the 0.5-percent average grade (combined copper and nickel) shown in figure 24 for the inverse distance squared method corresponds to 3.7 million short tons. The associated cutoff grade is 0.37 percent combined copper and nickel (fig. 23). Average copper grade is approximately 0.245 percent, and the average nickel grade is 0.255 percent. (See fig. 25.) Thus, in situ copper metal is about 9,070 short tons, and contained nickel metal is 9,440 short tons for these intervals.

The relation between average copper and nickel grades shown in figure 25 is different than that observed for block VIII, where average nickel grades generally exceed average copper grades. For each cutoff tonnage computed for block IV, the average nickel and copper grades are much closer in absolute value, and average copper grades actually exceed nickel for some tonnages.

Table 8 presents the tonnage estimates for the individual 25-foot intervals in block IV. The interpreted boundaries of each interval are presented in figures 12–15. Entries in table 8 denoted as C2A, C3A, and C4A are intervals located in areas c2a, c3a, and c4a shown in the eastern corner of figure 15. For example, tonnage indicated in table 8 in C2a includes the rock in the C2 interval in areas c2a, c3a, and c4a indicated on figure 15. These areas are the consequence of one drill hole in the eastern part of block IV which intersected a thick cordierite-rich metasedimentary rock interval. Even though this was a complicating factor, no drill holes were omitted because there were so few with which to work. Results presented in table 8 show ore tonnage declining as distance from the lithologic contact increases. The combined tonnages associated with layers C2A, C3A, and C4A are probably impractical to mine because of the large amount of waste rock that would have to be removed.

Even if these sections were minable, results of the inverse distanced squared calculations in table 8 show at a 0.4-percent cutoff grade, almost three-fourths of the rock in the delineated layers is waste. At a 0.2-percent combined cutoff grade, 13 percent of the rock is still waste.

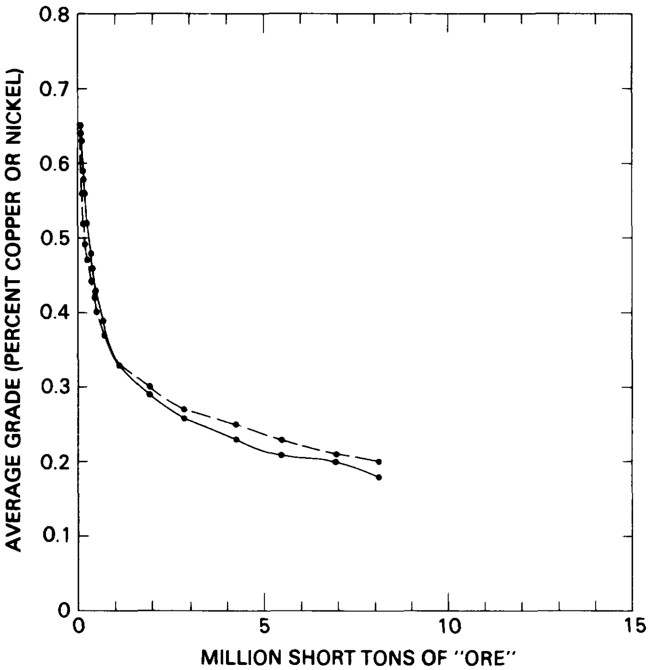

Figure 25. Average copper and average nickel grades vs. ore tonnage computed with the inverse distance squared algorithm for block IV. Mining blocks are 25×25×25 feet. Solid line represents copper. Dashed line represents nickel.

Again, the fraction of the waste rock to total rock increases with distance from the Basal series-metasedimentary rock contact.

IMPLICATIONS

A combined estimate of grade and tonnage for several areas of the Stillwater Complex has been presented in an earlier report (Dayton, 1971). By using computerized detailed copper- and nickel-concentration data from within the Mountain View area (from relevant drill holes) and a current geologic interpretation, we eliminated areas where extrapolation of grades was inappropriate or where there was insufficient data. The tonnage estimates for the blocks that were examined are still tentative due to assumptions made concerning continuity of mineralization. These estimates require validation by additional drilling in block IV and block VIII. The question of whether to focus drilling within the evaluated fault-bounded blocks or elsewhere depends on the commercial feasibility of mining a small deposit from the evaluated blocks. If additional tonnage is required for commercial development, future drilling should be focused in other blocks in rock units immediately above and below the lithologic contact between the Basal series and the cordierite-rich metasedimentary rock.

REFERENCES CITED

Briggs, Ian, 1974, Machine contouring using minimum curvature: Geophysics, v. 39, no.1, p. 39–48.

Dayton, Stanley, 1971, Hot air over Stillwater, profile of a hearing on mineral entry: Engineering and Mining Journal, v. 172, no. 10, p. 75–84.

Drew, L. J., Bawiec, W. J., Page, N. J, and Schuenemeyer, J. H., 1985, The copper-nickel concentration log—A tool for stratigraphic interpretation within the Ultramafic and Basal zones of the Stillwater Complex, Montana: Journal of Geochemical Exploration, v. 23, p. 117–137.

Dynamic Graphics, Inc., 1984, Interactive surface modeling: Berkeley, Calif.

Jackson, E. D., 1961, Primary textures and mineral associations in the Ultramafic zone of the Stillwater Complex, Montana: U.S. Geological Survey Professional Paper 358, 106 p.

Kleinkopf, M. D., 1985, Regional gravity and magnetic anomalies of the Stillwater Complex area, *in* Czamanske, G. K., and Zientek, M. L., eds., Stillwater Complex, Montana; Geology and guide: Montana Bureau of Mines and Geology, Special Publication 92.

Page, N. J, 1977, Stillwater Complex, Montana—Rock succession, metamorphism and structure of the complex and adjacent rocks: U.S. Geological Survey Professional Paper 999, 79 p.

———1979, Stillwater Complex, Montana—Structure, mineralogy, and petrology of the Basal zone with emphasis on the occurrence of sulfides: U.S. Geological Survey Professional Paper 1038, 69 p.

Page, N. J, and Dohrenwend, J. C., 1973, Mineral resource potential of the Stillwater Complex and adjacent rocks in the northern part of the Mount Wood and Mount Douglas quadrangles, southeastern Montana: U.S. Geological Survey Circular 684, 9 p.

Page, N. J, and Nokleberg, W. J., 1974, Geologic map of the Stillwater Complex, Montana: U.S. Geological Survey Miscellaneous Investigation Series Map I–797, 5 sheets, scale 1:12,000.

Zientek, M. L., 1983, Petrogenesis of the Basal zone of the Stillwater Complex, Montana: Ph.D. thesis, Stanford University, Palo Alto, California.

Zientek, M. L., Czamanske, G. K., and Irvine, T.N., 1985, Stratigraphy and nomenclature for the Stillwater Complex, *in* Czamanske, G. K., and Zientek, M. L., eds., Stillwater Complex, Montana; Geology and guide: Montana Bureau of Mines and Geology, Special Publication 92.

☆ U.S. GOVERNMENT PRINTING OFFICE 1987 - 181-407 - 226/40113

…VIEW AREA, STILLWATER COMPLEX, MONTANA—U.S. Geological Survey Bulletin 1674–B